14卷2期 地 震 工 程 与 工 程 振 动 Vol. 14, No. 2
1994年6月 EARTHQUAKE ENGINEERING AND ENGINEERING VIBRATION June, 1994

INFLUENCE OF THE GEOMETRY OF SEDIMENTARY BASINS ON THE FREQUENCY DEPENDENT DURATION OF STRONG EARTHQUAKE GROUND MOTION

by

Elena I. Novikova and M. D. Trifunac
(Dept. of Civil Eng., Univ. of Southern California,
Los Angeles, California, 90089—2531, U. S. A.)

ABSTRACT

This paper describes several empirical models of the duration of strong ground motion. We use the definition of druation of a function of motion $f(t)$, where $f(t)$ is acceleration, velocity or displacement, as the sum of time intervals during which the integral $\int_0^t f^2(\tau)d\tau$ gains a significant portion of its final value. All the records were band - pass filtered through 12 narrow filters and the duration of the strong ground motion was studied separately in these frequency bands. In addition to the "traditional" parameters, such as the earthquake magnitude and the epicentral distance, three other parameters, which describe the geometry of the sedimentary basins surrounding the recording stations, are considered. It is shown how the presence of sediments prolongs the duration at some frequencies. This prolongation can be approximated by a coupled quadratic function of the depth and the width of the sedimentary valley, and by a linear function of the angle, subtended at the station by the rocks, which reflect seismic waves towards the station. The maximum prolongation occurs for moderate depths ($2 \div 3$km) and widths ($30 \div 50$km) of the sediments. The additional duration can be as much as $6 \div 7$ sec at frequencies near 1Hz. Studies of the length and of the number of the strong motion intervals, contributing to the overall duration of strong motion, show that this additional duration may be interpreted to result from multiple reflection of waves from the bottom and from the edges of the sedimentary valleys.

INTRODUCTION

Duration of strong ground motion characterizes the rate of the energy input to a structure and must be considered, especially for the analysis of a nonlinear response. Duration of strong motion also plays a significant role in the response of soils to an earthquake excitation in determination whether the liquefaction or permanent soil displacement are possible. Thus, understanding the

causes for the prolongation of duration of shaking at some sites is important for successful and realistic analyses of the response of soils and structures.

In this paper, we review several empirical regression equations of the duration of strong earthquake ground motion in terms of the earthquake magnitude, M, the epicentral distance, Δ, and the region specific propagation parameters. We study the duration of strong ground motion in 12 frequency bands, here called channels, with central frequencies ranging from $f_0=0.075$Hz to $f_0=21$Hz. Band-pass filtering is applied to 486 vertical and 984 horizontal components of acceleration, velocity and displacement, generated by 106 earthquakes and recorded at 267 sites in the Western U. S. (Lee and Trifunac, 1987). The distribution of good quality 3-component records in this database with respect to earthquake magnitude and epicentral distance is shown is figure1. At each channel, only carefully selected data, which have high signal to noise ratio, were used in the analysis (figure 2), and the durations of acceleration, velocity and displacement were considered as one homogeneous data set (Novikova and Trifunac, 1993a).

In each frequency band, we define the strong motion parts of a function $f(t)$ as those time intervals during which the integral $\int_0^t f^2(\tau)d\tau$ has the steepest slope and gains 90% of its final value (figure 3). The sum of those time intervals is called the "observed" duration of strong motion. Other physically related definitions of duration (McCann and Shah, 1979; Vanmarcke and Lai, 1980) do not allow for the strong motion part to consist fo several portions or do not give the specific position of the strong motion portion in the record. The important feature of the definition we use is that it is of the "relative" type, i. e. it does not include information about the absolute level of acceleration, while the "absolute" definitions, like the one of Page et al. (1972) do carry this information. The knowledge of the frequency dependent duration in this "relative" sense combined with the information about the Fourier spectral amplitudes (Trifunac, 1989a, b, c; 1991) at all frequencies provides a fairly complete description of the strong motion.

Several empirical models which scale the duration in terms of the magnitude, the epicentral distance and other parameters are available in the literature (Trifunac and Brady, 1975; Trifunac and Westermo, 1977; 1982; Westermo and Trifunac, 1978; 1979; Novikova and Trifunac, 1993a, b, c). In this paper, we consider new, more detailed models which use a new characterization of the recording site conditions. The purpose of this study is also to improve our understanding of the nature of the wave propagation in the highly inhomogeneous media of the upper crust.

PARAMETERS, INVOLVED IN THE REGRESSION MODELS

We consider the duration of strong ground motion as the sum of three terms:

$$dur = \tau_0 + \tau_\Delta + \tau_{region} \tag{1}$$

where dur is the total duration of acceleration, velocity or displacement, τ_0 stands for the duration of the rupture process at the source, τ_Δ represents the increase in duration due to propagation effects and τ_{region} describes the prolongation effects caused by the geometry of the regional geologic features. We model the dependence of τ_0 on magnitude M by a quadratic function of M: $\tau_0 \approx a_1 +$

$a_2 \cdot M + a_3 \cdot M^2$, where $a_i (i = 1 \div 3)$ are unknown coefficients. We prefer this quadratic expression over more "natural" exponential function because of two reasons (Novikova and Trifunac, 1993a). First, exponential dependence of the rupture time on frequency holds only for relatively high frequencies, since any source can be represented as a point (delta - function in space and time) when observed through long - wave - length window. At these low frequencies, the rupture time cannot be observed (at least using the "relative" type of the definition of duration), and, thus, should not depend on M at all. Second, exponential dependence of τ_0 on M results in nonlinear regression analysis, which, generally, is not stable, especially for small number of data points. The second term in eq. (1), τ_Δ, is modeled by a linear function of the epicentral distance $\tau_\Delta(f) = a_4(f) \cdot \Delta$, because this form is consistent with the data (Novikova and Trifunac, 1993a) and agrees with the interpretation that the duration of strong motion increases with the distance traveled due to dispersion of the strong motion waves. Multiple window Fourier analysis shows that even for small epicentral distances the prime carrier of the strong motion energy are surface waves (Trifunac, 1971a).

The sum $\tau_0 + \tau_\Delta$ represents duration observed at the sites located on basement rock and is called here "basic duration." It serves as a basis for developing more "complete" models accounting for prolongation of duration at the sites located on sediments. In this paper, we consider the influence of the geometry of the sedimentary basin by assuming a special form of the term τ_{region} in eq. (1).

Deviations from a uniform horizontally layered curst model occur everywhere along the path of the waves propagating from the fault to the recording site. For the San Fernando, 1971, California, earthquake, which generated large percentage of the accelerograms in our database, substantial deviations from a multilayered model dominate in the whole region shaken by this event. These deviations occur due to the topography of the basement rock, so that the several upper kilometers of the earth's crust can be viewed as a collection of sedimentary basins separated by irregularly shaped basement rock barriers. These "barriers" can be recognized on the surface as mountains, coupling geological and topographical irregularities (figure 4). The influence of such structures on the propagating waves can be understood by studying idealized sedimentary basins (Trifunac, 1971b; 1973; Wong and Trifunac; 1974a, b; Todorovska and Lee, 1990; 1991a, b), by generalization of the solutions to arbitrary shaped layers (Moeen－Vaziri and Trifunac, 1988a, b), and by interpretation of recorded data and numerical modeling of the wave propagation (Vidale and Helmberger, 1988).

The ability of the basement rocks surrounding a sedimentary valley, to reflect waves back into the valley, and the conversion of incident body waves into "surface" waves at the boundaries of a sedimentary basin, leads us to assume that some parameters describing the characteristic horizontal dimension of these sedimentary basins should play a role in the description of the duration of strong ground motion. We will explore the resulting prolongation of the duration at the stations which are situated on sedimentary deposits by considering two parameters. One of those is the horizontal distance R (figures 5－7) from the station to the nearest basement rock appearing on the surface and producing reflections. We choose the second parameter, φ, to describe the "efficiency".

of these reflections (figures 5—6). The angle with which the reflecting surface of the rocks can be seen from the station is one such measure of the "efficiency"of the secondary (reflected) waves.

Only a part of the boundary between the rock and the sediments which receives direct waves from the source will be capable of generating reflected waves and will be considered in the determination of R and φ (figure 5). Thus there are several "distances"from the rock to the station to be considered. For example:the shortest distance,the distance to the middle of the reflecting surface and so on. Our"R"was chosen to be such a distance from the rock to the station ,which gives the shortest possible path source—rock—station.

The station may be surrounded by several rocks (or clusters of rocks),capable of producing reflections. We consider the hypothetical geometry,shown in figure 5. Two "rocks"are located in the vicinity of the source and the station. The direct waves from the source can be reflected in the direction of the station,causing prolongation of the duration of the strong ground motion there. We designate the distance from the source to the $i\overset{th}{-}$ rock as r_i,and the distance from the $i\overset{th}{-}$rock to the station as R_i. The angles,subtended at the recording station by the surfaces of the $i\overset{th}{-}$rock, we designate as φ_i We wish to combine the individual parameters R_i and φ_i into some "overall"R and φ ,which would characterize all the rocks as a group.

First,we consider the "energy equation,"which would relate the energy of the waves reflected by individual rocks towards the station. Taking the density of the energy emitted by the source in frequency f as 1,we have for the density of the energy,arriving to the $i\overset{th}{-}$ rock

$$\frac{1}{r_i^n}\exp\left(\frac{-2\pi f r_i}{Qv}\right),$$

where Q designates the quality factor,$n=1$ (for surface waves) or $n=2$(for body waves),and v stands for the velocity of the waves. The energy reflected from the $i\overset{th}{-}$ rock in the direction of the station is assumed to be proportional to the length of the reflecting surface of this rock,$R_i\varphi_i$ The energy,which comes to the station after being reflected by the $i\overset{th}{-}$ rock is then proportional to

$$\frac{1}{R_i^n}\exp\left(\frac{-2\pi f R_i}{Qv}\right)R_i\varphi_i\cdot\frac{1}{r_i^n}\exp\left(\frac{-2\pi f r_i}{Qv}\right)$$

The "overall"R and φ should represent some "fictitious"rock which alone can reproduce the same effect as the combination of several rocks we are considering. The energy reflected by this "fictitious" rock alone should be the same as all the energy reflected by the group of individual rocks:

$$\exp\left\{\frac{-2\pi f}{Qv}(R+r)\right\}\cdot\frac{R\varphi}{R^n r^n}=\sum_i\exp\left\{\frac{-2\pi f}{Qv}(R_i+r_i)\right\}\frac{R_i\varphi_i}{R_i^n r_i^n}\quad\} \tag{2}$$

The above "energy equation,"however,is too complex to be considered in the present exploratory analysis. It has many parameters and accounts for effects which may be overshadowed by other unknowns. Thus,we will disregard the geometrical spreading,because the size of the source and the length of the reflecting surfaces of the rocks can be assumed to be large compared with the epicentral distance and with the distances R_i and r_i. We will also disregard the attenuation factor, Q. We,recognize,however,that the attenuation of the secondary pulses (reflected from the rocks)

may play a significant role in the formation of the strong motion parts of the record. We will account for the attenuation later, by assuming a special shape of the functional dependence of the duration of the strong ground motion on R. Without geometrical spreading and without attenuation, the "energy equation"(2)simplifies to

$$R\varphi = \sum_i R_i \varphi_i \tag{3}$$

which states that the reflecting surface of the "fictitious"rock should be equal to the sum of the reflecting surfaces of the individual rocks.

We next consider the "delay equation. "The pulse, reflected by a rock in the direction of the station, spends more time in the medium (than the direct pulse), when it travels the distance $R_i + r_i$, and arrives at the station later. The "fictitious"rock has to be positioned at such a distance R from the station, that the delay of the pulses, coming from it , represents some "proper"combination of the delays of pulses, coming from the individual rocks. The time, when the pulse from the "fictitious"rock should be expected at the recording station, $(R+r)/v$, can be approximated as a weighted sum of the times of the arrivals of the individual pulses, $(R_i+r_i)/v$. The weight of each individual pulse can be assumed to be proportional to the portion of energy it delivers to the station when compared to the total energy brought to this station by all the reflected pulses:

$$\frac{R+r}{v} = \sum_i \left\{ \frac{R_i + r_i}{v} \left[\frac{\exp\left\{ \frac{-2\pi f}{Qv}(R_i + r_i) \right\} \cdot \frac{R_i \varphi_i}{R_i^n r_i^n}}{\sum_j \left(\exp\left\{ \frac{-2\pi f}{Qv}(R_i + r_i) \right\} \cdot \frac{R_j \varphi_j}{R_j^n r_j^n} \right)} \right] \right\} \tag{4}$$

After disregarding the geometrical spreading and attenuation, the "delay equation"(4)simplifies to

$$\frac{R+r}{v} = \sum_i \frac{R_i + r_i}{v} \cdot \frac{R_i \varphi_i}{\sum_j R_j \varphi_j}$$

The times of the individual arrivals are weighted now according to the length of the reflecting surfaces of the rocks, $R_i \varphi_i$. The velocity can be factored out from the above equation if the properties of the sediments in the region are assumed to be homogeneous. Next, we assume that the distance from the source to the "fictitious"rock, r, and all the distances from the source to the individual rocks are comparable, i. e. $r \approx r_i$ for all i. Recaling the identity

$$r = \sum_i r \frac{R_i \varphi_i}{\sum_j R_j \varphi_j},$$

we get the simplified "delay equation":

$$R = \sum_i R_i \frac{R_i \varphi_i}{\sum_j R_j \varphi_j}. \tag{5}$$

We note, however, that eqs. (3)and (5) were not used directly, when the measurements of R and φ were carried out. Instead, we used the physical intuition and common observational sense. which were based on and guided by the above considerations.

Some examples of the determination of the parameters R and φ are shown in figure 6. In many cases a considerable uncertainty is involved in the process of selecting specific values for R and φ. For example, which rocks should be considered as potential reflectors? This depends on the distances to the different rocks, on their location relative to the source, to the station and to each other, their horizontal dimensions, magnitude of the earthquake, depth of the hypocenter and rate of attenuation of strong motion with distance (Trifunac and Lee, 1990) and ……the intuition of the investigator.

Next we consider the strong ground motion as it is seen at the recording station, located in a sedimentary basin and surrounded by rocks. Direct P -, S - and surface waves are arriving to the station first, and those generate strong ground motion of some duration. Later, some reflected, scattered and other delayed waves arrive. Many of those do not have amplitudes that are big enough (compared to the direct wave amplitudes) and so do not cause significant increase of the initial duration of strong motion. However, some of those "late" waves, reflected by well - defined boundaries between the sediments and the basement rock, significantly differ from other scattered waves. These waves cause additional pulses which will contribute to the duration of strong motion energy observed at the station. The above simple physical considerations allow us to search for the functional form of the dependence $\tau_{region} = \tau_{region}(R, \varphi)$.

We first discuss the dependence of τ_{region} on the angle φ. We recall that φ is a measure of the "efficiency" of the reflections. If this angle is small, the reflected wave carries little energy and cannot be noticed relative to the background of the other waves. The increase of φ leads to an increase of the duration of the reflected pulses, because large φ implies long reflecting surface and increases the variety of the sampled lengths of the propagation paths source - rock - station. These considerations suggest that τ_{region} is an increasing function of φ. The data presently available (Novikova and Trifunac, 1993a) suggest that the dependence of τ_{region} on φ can be approximated by a linear function.

The dependence on R is more complex. Suppose first that R is small. Then the time intervals which correspond to the initial pulse (of duration dur_1) and to the reflected pulse (of duration dur_2) will be observed at the station almost simultaneously, without producing significant increase in the duration. Next, consider larger R. The time delay between the two pulses of energy causes the complete separation of the corresponding intervals of strong motion, and the total duration is longer now and equal to $dur_1 + dur_2$. Further increase of R causes an increase of the time which the reflected waves spend travelling through a dispersive medium. This causes increase of dur_2 and results in further prolongation of the total duration $dur_1 + dur_2$. Finally, consider that R is big. The second pulse, generated by reflection from a remote rock, experiences strong attenuation and is so weak now that it cannot be noticed relative to the background of the scattered waves. The further the rock is, the weaker the pulse will become. Therefore, two ranges of horizontal characteristic dimension (distance to the reflecting rock) exist: "small" R, where duration of strong motion grows with increasing R, and "large" R, where the effect is just the opposite. The simplest way to describe such dependence on R is to use a parabolic function,

$$\tau_{region}(R) = const_1 + const_2 \cdot R + const_3 \cdot R^2 \tag{6}$$

where $const_i, i=1,2,3$ are constants (different at different frequency bands), and we expect that $const_3<0$.

Next consider the depth of the sedimentary deposits at the recording site, h. It has been recognized that the parameter h plays an important role in scaling various characteristics of strong earthquake ground motion (Trifunac, 1989a; 1991; Trifunac and Lee, 1990; Lee, 1991). Some studies on the influence of the depth of sediments on the duration of strong motion were also performed (Westermo and Trifunac, 1978; 1979; Trifunac and Westermo, 1982). In the last group of papers, the linear dependence $\tau_{region}(h)=const_4+const_5 \cdot h$, where $const_4$ and $const_5$ are frequency dependent regression coefficients, was considered. In the present study, we will assume the parabolic dependence

$$\tau_{region}(h) = const_4 + const_5 \cdot h + const_6 \cdot h^2, \tag{7}$$

where $const_i$ i=4,5,6 are frequency dependent coefficients. The reason for this is that the dependence $\tau_{region}(h)$ should be similar to $\tau_{region}(R)$ with the difference in scale, due to the fact that h describes the dimension perpendicular to the predominant direction of the strong motion wave propagation.

How should eqs. (6)-(7) be combined to describe the prolongation of the duration at a station located on sediments of the depth h and at distance R from the edge of the valley? Consider the wave travelling from the valley towards the edge of the sedimentary deposits (figure 7). The wave cannot penetrate all the way to the edge of the basin, and reflects back into the valley before reaching the surface boundary of the rocks and the sediments. The length of this "penetration" depends on the geometry of the basin, on the wavelength of the wave and on the incident angle. We introduce here the "effective" horizontal distance R_{eff}, that is the distance from the station to the region of reflection. It is the parameter R_{eff} which should be considered in eq. (6) instead of R. R_{eff}, however is hard to determine, and so we use only R and h in our equations and account for the existence of the "effective" horizontal distance R_{eff} via empirical regression coefficients. By fixing the horizontal dimension, R, and by changing the depth of the sediments, h, one changes R_{eff}. This means that the effects produced by parameters R and h are related to each other. The appropriate way to account for this coupling is to combine eqs. (6) and (7) and add one more, coupling, term:

$$\tau_{region}(R,h) = const_1 + const_2 \cdot R + const_3 \cdot R^2 + const_4 + const_5 \cdot h + const_6 \cdot h^2 + const_7 \cdot Rh. \tag{8}$$

The constant term $const_1+const_4$ in $\tau_{region}(R,h)$ should be equal to zero, because no prolongation of the duration (of the type discussed above) is possible when $R=h=0$ (which simply means that the station is on basement rock). Renaming the coefficients in eq. (8), and recalling the contribution from the angle of reflection φ, the final form of $\tau_{region}(R,h,\varphi)$, in this study, becomes:

$$\tau_{region}(R,h,\varphi) = \tau_{region} = a_5 \cdot h + a_6 \cdot R + a_7 \cdot hR + a_8 \cdot R^2 + a_9 \cdot h^2 + a_{10} \cdot \varphi \tag{9}$$

Here a_i, i=5÷10 are some unknown coefficients. This numbering of the coefficients was chosen to maintain consistency with our previous work (Novikova and Trifunac, 1993a). Note that the sum of the first five terms in eq. (9) corresponds to the complete decomposition of the dependence τ_{region}

$= \tau_{region}(R,h)$ as a function of two variables into Taylor series up to the second order (assuming the constant term is zero).

THE REGRESSION MODELS

Several models of the duration of strong ground motion are presented in this section. The unknown coefficients of each model were obtained from linear regression analysis, performed separately at each channel. The singular value decomposition method (Press et al., 1986) was used to maintain good control over the accuracy of the inversion problem.

The regression models are constructed starting with the "basic"model, which scales the duration of strong ground motion in terms of the earthquake magnitude and the epicentral distance. In addition to the terms τ_0 (duration of the source radiation) and τ_Δ (prolongation due to the propagation effects), which are both included in the "basic"model, we consider the prolongation of the duration represented by the term τ_{region} in eq. (1). First we present the model which uses the most "complete" form of this term, given by eq. (9). A discussion of the regression coefficients, resulting from this model will follow. Then, two other, "truncated," forms of the term τ_{region} will be given for the models, which can be used when not all of the parameters h, R and φ are known.

Model $dur = dur(M, M^2, \Delta, h, R, hR, R^2, h^2, \varphi)$

The most "complete"model among all of the ones studied in this work includes the dependence on magnitude M and on epicentral distance Δ as in the "basic"model. It also includes the dependence of the duration on the depth of sediments at the recording site, h, on the characteristic horizontal distance to the rocks, capable of reflecting seismic waves towards the station, R, and on the angle φ, subtended at the station by the surface of the reflecting rock. The regression equation of this model is:

$$\begin{Bmatrix} dur^{(h)}(f) \\ dur^{(v)}(f) \end{Bmatrix} = \begin{Bmatrix} a_1^{(h)}(f) \\ a_1^{(v)}(f) \end{Bmatrix} + a_2(f) \cdot \overline{M} + a_3(f) \cdot \overline{M}^2 + a_4(f) \cdot \Delta +$$

$$+ \begin{Bmatrix} [a_5^{(h)} \cdot h + a_6^{(h)}(f) \cdot R + a_7^{(h)}(f) \cdot hR + a_8^{(h)}(f) \cdot R^2 + a_9^{(h)}(f) \cdot h^2 + a_{10}^{(h)}(f) \cdot \varphi]_+ \\ [a_5^{(v)} \cdot h + a_6^{(v)}(f) \cdot R + a_7^{(v)}(f) \cdot hR + a_8^{(v)}(f) \cdot R^2 + a_9^{(v)}(f) \cdot h^2 + a_{10}^{(v)}(f) \cdot \varphi]_+ \end{Bmatrix}, \tag{10a}$$

where the epicentral distance, Δ, the depth of sediments, h, and the distance to the reflecting rock, R, are measured in kilometers. The angle φ is measured in degrees and

$$\overline{M} = \max\{M, M_{min}(f)\}, \qquad M_{min}(f) = \frac{-a_2(f)}{2a_3(f)} \tag{10b}$$

$\overline{M}$ is introduced to keep the duration of strong ground motion a nondecreasing function of magnitude (Novikova and Trifunac, 1993a). The expression in the square brackets in eq. (10a) represents the frequency dependent term τ_{region} when it is given by eq. (9), and

$$[\tau_{region}(f)]_+ = \max\{0, \tau_{region}(f)\} = \begin{cases} \tau_{region}(f), & if \quad \tau_{region}(f) > 0, \\ 0 & \text{otherwise} \end{cases} \tag{10c}$$

The values of R, h and φ are assumed to be zero if the station is located on rock.

Preliminary analysis shows that the constant term a_1 and the dependence of the duration of strong motion on the parameters h, R and φ is different for the horizontal and for the vertical components. Therefore we consider two different sets of coefficients, $\{a_i^{(h)}(f), i=1,5\div10\}$ for the horizontal components, and $\{a_i^{(v)}(f), i=1,5\div10\}$ for the vertical ones.

The regression analysis using eq. (10) is accomplished in three steps, two of which are the same as those for the "basic" model (Novikova and Trifunac, 1993a). During the first step, we assume $\overline{M}=M$ and disregard the subscript "+" of the term τ_{region} in eq. (10a). The regression coefficients obtained so, allow one to evaluate $M_{min}(f)$ using eq. (10b), and to proceed to the second iteration, which accounts for the nondecreasing nature of the dependenceof the duration on magnitude. During the third iteration, the previously obtained coefficients are used in the evaluation of the term τ_{region}, so that eq. (10c)can be used, and only the positive contribution of τ_{region} is taken into account. Remarkably, all three sets of coefficients, obtained in those three iterations, are very similar. This results from the fact that just a few data points have $M<\overline{M}$ or $\tau_{region}<0$.

Table 1 presents the results of the regression analysis of eq. (10). The regression coefficients are given as $a_i(f)\pm\sigma_i(f)$, where $\sigma_i^2(f)$ are the variances of the values found. Zero values for the coefficients correspond to the cases when $|\sigma_i/a_i|>1$. Figure 8 displays the dependence of the coefficients of the regression model on frequency (solid lines) and shows their reliability in terms of the "σ-interval" and the 95% confidence interval. the coefficients $\{a_i(f), i=1\div4\}$ show how the duration depends on the magnitude and on the epicentral distance. At the first channel, no dispersion is noticed (at the distances where the motion is still strong) due to the existence of only one mode of the surface waves. At other channels, the duration of strong motion increases with distance, due to dispersion (Novikova and Trifunac, 1993a) (at low and intermediate frequencies) and due to scattering (at high frequencies). No dependence of the duration on magnitude M can be detected at low frequencies, because the dimension of the source is smaller than the wavelength of the seismic waves at these frequencies. As the frequency increases, first linear, and then quadratic dependence on M can be observed. A more detailed discussion of these effects can be found in our previous work (Novikova and Trifunac, 1993a).

The coefficients $\{a_i(f), i=5\div10\}$ describe the influence of the geometry of the sedimentary basin where the recording station is located. The coefficient $a_{10}(f)$ represents the "strength" of the horizontal reflections (measured by the angle φ), and it is positive. The coefficients scaling the contribution of the quadratic terms R^2 and h^2 are negative, as expected. Thus, the description of the prolongation of the duration by the presence of a sedimentary basin results in the increase of duration for the intermediate values of R and h and in no increase for small or large R and h. Figure 9 shows isolines (in seconds) of the positive contribution to the overall duration, predicted by eq. (10), made by the following sum of terms, involving R and h:

$$\begin{Bmatrix}\tau_{region}^{(h)}(R,h)\\ \tau_{region}^{(v)}(R,h)\end{Bmatrix}=\begin{Bmatrix}a_5^{(h)}\cdot h+a_6^{(h)}\cdot R+a_7^{(h)}\cdot hR+a_8^{(h)}\cdot R^2+a_9^{(h)}\cdot h^2\\ a_5^{(v)}\cdot h+a_6^{(v)}\cdot R+a_7^{(v)}\cdot hR+a_8^{(v)}\cdot R^2+a_9^{(v)}\cdot h^2\end{Bmatrix}. \tag{11}$$

Figure 9 also shows the observed duration, which is presented averaged over the ranges of R and h. The darker shade corresponds to longer observed duration. The same scale of shades is chosen for the horizontal and for the vertical components of each channel, but different frequency bands

have different scales. No shade corresponds to the ranges of R and h where no data are available. For both horizontal and vertical components, practically all the data points fall in the area where $\tau_{region}(R,h)>0$. Consequently, $\tau_{region}(R,h,\varphi)=\tau_{region}(R,h)+\{$contribution by $\varphi\}$is greater than zero for even greater number of data points. This not only explains why the third iteration of the model (which treated the points where $\tau_{region}<0$ in a special way) and the second iteration (which did not consider condition (10c)) gave practically the same results, but also verifies our approximate assumptions about how the presence of a sedimentary basin can influence the duration of strong ground motion.

The coefficients representing the prolongation of the duration of the strong ground shaking by the specific shape of the valley are distinct from zero in the intermediate frequency range only. To explain this, we consider here the model proposed by Trifunac (1990) for the description of the effects produced by geological sediments and local soils on the amplification of strong motion. According to this model, a layer of sediments of thickness h works as a band-pass amplificafion filter with specific high, f_1 and low, f_2 cut-off frequencies. The low cut-off is the frequency for which the corresponding quarter wavelength in sediments coincides with the thickness of sediments, h. The high cut-off depends, among other parameters, on the attenuation factor Q, typical for the sediments considered. For high frequencies, the amplification effects compete with the inelastic attenuation. In the intermediate range $f_2>f>f_1$, the average amplification practically does not depend on frequency. The amplification effects can be explained by multiple reflections inside the sedimentary basin (an increase in waveamplitude upon entering the soft layer also takes place). The physical reason that leads to prolongation of the duration in a sedimentary valley can be assumed to be the same multiple reflection phenomenon. One of the "geology"models, used for description of the amplification effects (Trifunac, 1990) had the following parameters: depth of sediments $h=2$km, shear wave velocity $\beta=2$km/sec, and inelastic attenuation parameter $Q=100$. The estimates of $f_1$and $f_2$came out to be: for the high cut-off frequency $f_1=5$Hz, and for low cut-off $f_2=0.24$Hz. A good agreement can be found between these values of f_1 and f_2 and the frequencies that bound the range where the prolongation of the duration due to the presence of a sedimentary basin can be seen.

At low frequencies ($f\leq 0.3$Hz), all the coefficients $\{a_i(f), i=5\div 10\}$are equal to zero and no influence of the sedimentary basin on the duration of motion can be noticed. At channel #4 ($f_0=0.37$Hz), the prolongation of the duration is expressed by the term involving φ only (see table1.) The angle of effective reflection, φ, appears to be more sensitive to long waves than the parameters R and h, because it measures the overall "strength of reflection"(without going into details of the geometry).

At $f=0.63\div 2.5$Hz, the geometrical properties of the sedimentary basin "work"in full strength, and all the terms in τ_{region}have non-zero values. It is interesting to notice that the range of parameters R and h where $\tau_{region}(R,h)>0$ (the area inside the zero isoline in figure 9), being slightly different for the horizontal than for the vertical components, preserves itself for both components in the frequency range $f=0.63\div 2.5$Hz. This effect may be similar in nature to the effect of absence of dependence of the amplification factor on the frequency of motion inside the interval

$f_2<f<f_1$(Trifunac, 1990). Inside the frequency range where $\tau_{region}(R,h)>0$, the value of $\tau_{region}(R,h)$, however, does depend on frequency. The maximum possible contribution of $\tau_{region}(R,h)$ changes from 7.5sec to 2.5 sec for the horizontal components, and from 5 sec to 3.5 sec for the vertical component, when the frequency changes from 0.63Hz to 2.5Hz. The difference in prolongation for different frequencies might be interpreted by the hypothesis that longer waves will cause longer prolongation of the duration simply due to their long period nature.

After the transition range (4.2÷7.2Hz), where some effects of the geometry of the sedimentary basin can still be noticed, the short wave range ($f\geq$5.0÷8.5Hz)sets in. For these frequencies, no influence on the duration of strong ground motion by the presence of a sedimentary basin with specific geometry can be observed. This could be explained by the high inelastic attenuation, typical for the upper hundreds of meters of soil and sediments. In Pliocene - Pleistocene sediments of the Los Angeles basin, Hauksson et al. (1987)estimated Q for shear waves to be in the range from 25 to 100 for depths between the surface and 1500m. Malin et al. (1988) observed and average $Q=9$ for shear waves in an ophiolite complex at Oroville, valid for depths from 0 to 500m. So, for high frequencies, multiple reflections, causing prolongation of the duration, have to compete with the inelastic attenuation, and the resulting effect appears to be negligible.

We examine now the differences between the sets of coefficients obtained for the horizontal $\{a_i^{(h)}(f), i=5\div10\}$and vertical $\{a_i^{(v)}(f), i=5\div10\}$components. The coefficients $a_6^{(h)}(f)$ and $a_8^{(h)}(f)$, which scale the influence of the parameter R on horizontal component of motion, are better defined and can be followed in a wider frequency range than their vertical counterparts $a_6^{(v)}(f)$ and $a_8^{(v)}(f)$. Conversely, the coefficients that describe the contribution of the depth of sediments h to the duration of the horizontal component, $a_5^{(h)}(f)$ and $a_7^{(h)}(f)$, have larger variances and are distinct from zero in a narrower frequency range compared to $a_5^{(v)}(f)$ and $a_7^{(v)}(f)$, which are responsible for the similar description in the case of the vertical components. As a result, the strong motion duration of the horizontal components appears to be more sensitive to the horizontal characteristic dimension R, while the duration of the vertical component "feels" the depth of sediments under the station, h, better than it "feels" R. If we assume that the Love waves, and the multiply scattered SHwaves, give more contribution to the horizontal component than to the vertical, and that the Rayleigh waves do produce a substantial vertical motion, then the asymmetry in the behavior of R - and h - related coefficients could be explained as follows. The parameter R describes the geometry of the basin on a large scale, while h gives a more local description in terms of the depth of sediments right under the recording station. the dispersion of the Love waves might be more sensitive to the "irregularities" in the layered media, than that of the Rayleigh waves (Levander, 1990). Our irregularly shaped reflecting rocks, positioned at distance R from the station, might be interpreted as such "irregularities." The dispersion of the Rayleigh waves, perhaps, does not "feel" the smooth irregularities in a wave guide that much , and , thus, the Rayleigh wave "carries" less information about R. Instead, this wave can be considered as a representative of the mean structure beneath the receiving station. This structure can be characterized by the depth of sediments at the recording site, h. So , simplifying, we might assume that the Love waves appear to carry information about the parameter R, and this information is recorded

predominantly by the horizontal components. The Rayleigh waves have substantial vertical component and "remember" the depth of sedimentary deposits, h, causing the duration of the vertical motion to be more sensitive to h.

There is also another reason why the strong motion duration of the vertical components is more sensitive to the depth of sediments than is the duration of horizontal strong motion. The duration of the vertical component of strong motion receives contributions from body P (and SV) waves (Novikova and Trifunac, 1993a). The P-arrival is seen on the horizontal components also, but it does not bring enough energy to be counted as strong motion. As a result, the information about the depth of sediments, carried by the P-wave and the waves scattered and reflected several times in the sedimentary layer just underneath the station, can be recognized primarily by the vertical component of motion.

The angle φ with which the reflecting rocks are "seen" from the station, is a measure of the contributions to the duration from the horizontal reflections. The characteristic "dimension" of these reflections is described by R. Both φ- and R-related coefficients are better defined for the horizontal components. The typical values obtained for $a_{10}(f)$ give an increase in duration by about 2 sec for $f \approx 0.37 \div 1.1$Hz and by about 0.5 sec and less for $f \approx 2.5 \div 4.2$Hz, per each 100° of φ.

Models $dur = dur(M, M^2, \Delta, R, R^2, \varphi)$ and dur = dur(M, M², Δ, h, h²)

It is not always possible to obtain information on all the parameters involved in the description of a sedimentary basin for the model (10). We will describe here two models that can be used if only h or only R and φ are available.

Consider first the model

$$\begin{Bmatrix} dur^{(h)}(f) \\ dur^{(v)}(f) \end{Bmatrix} = \begin{Bmatrix} a_1^{(h)}(f) \\ a_1^{(v)}(f) \end{Bmatrix} + a_2(f) \cdot \overline{M} + a_3(f) \cdot \overline{M}^2 + a_4(f) \cdot \Delta + \\ + \begin{Bmatrix} [a_6^{(h)}(f) \cdot R + a_8^{(h)}(f) \cdot R^2 + a_{10}^{(h)}(f) \cdot \varphi]_+ \\ [a_6^{(v)}(f) \cdot R + a_8^{(v)}(f) \cdot R^2 + a_{10}^{(v)}(f) \cdot \varphi]_+ \end{Bmatrix} \tag{12a}$$

where the epicentral distance, Δ, and the horizontal characteristic dimension, R, are measured in kilometers and φ is measured in degrees,

$$\overline{M} = \max\{M, M_{\min}(f)\}, M_{\min}(f) = \frac{-a_2(f)}{2a_3(f)} \tag{12b}$$

and

$$[\cdot]_+ = \max\{0, [\cdot]\}. \tag{12c}$$

The values of R and φ are assumed to be zero if the recording station is located on basement rock. The terms with superscript (h) correspond to the horizontal components and the terms with superscript (v) describe the vertical motion.

Eq. (12) was fitted to the data in three steps (identical to those described earlier for eq. (10). Table 2 shows the number of data points available, $N(f)$, all the fitted coefficients $a_i(f)$ and their variances $\sigma_i(f)$, $M_{\min}$, the average duration dur_{av} and the standard deviation σ_{dur} for each frequency band. Comparison with Table 1 shows that all coefficients, involved in this "truncated" model, are similar to their counterparts from the "complete" model (eq. (10)).

Figure 10 displays the positive contribution of the terms $a_6(f) \cdot R + a_8(f) \cdot R^2$ to the total duration, predicted by eq. (12), for horizontal and vertical motions. In the "truncated" model, where the geometry of the basin is described by R only (instead of by R and h, as it is done in the "complete" model), the result appears to be "averaged" over the depth of sediments h.

The second "truncated" model, considered in this paper, addresses the case when only the depth of sediments, h, is available:

$$\begin{Bmatrix} dur^{(h)}(f) \\ dur^{(v)}(f) \end{Bmatrix} = \begin{Bmatrix} a_1^{(h)}(f) \\ a_1^{(v)}(f) \end{Bmatrix} + a_2(f) \cdot \overline{M} + a_3(f) \cdot \overline{M}^2 + a_4(f) \cdot \Delta + \\ + \begin{Bmatrix} [a_5^{(h)}(f) \cdot h + a_9^{(h)}(f) \cdot h^2]_+ \\ [a_5^{(v)}(f) \cdot h + a_9^{(v)}(f) \cdot h^2]_+ \end{Bmatrix} \tag{13a}$$

where the epicentral distance, Δ, and the depth of sediments under the recording site, h are measured in kilometers,

$$\overline{M} = \max\{M, M_{\min}(f)\}, M_{\min}(f) = \frac{-a_2(f)}{2a_3(f)} \tag{13b}$$

and

$$[\cdot]_+ = \max\{0, [\cdot]\}. \tag{13c}$$

The results of the regression analysis are shown in table 3 and in figure 11. As before (see "complete" model, eq. (10)), the vertical component is more sensitive to the depth of sediments, than the horizontal one.

Distribution function of the residuals

To get an estimate of the probability with which any given duration of shaking will be exceeded during an earthquake with given parameters at a site with known properties, we studied the residures of the models presented. We considered the relative residuals, $\lambda = dur_{obs}/dur$, were dur_{obs}/dur is the observed duration, and dur is the duration, predicted by a model. We found that the distribution function of λ is very similar for the different models and for the different frequency bands, and that it can be approximated by the function

$$q(\lambda) = \frac{1}{\eta} \cdot \frac{\lambda^b}{a + \lambda^c} \tag{14a}$$

where η is the normalizing coefficient:

$$\eta = a^{\frac{b+1}{c}-1} \cdot \frac{\pi}{c} \cdot [\sin \frac{(b+1)\pi}{c}]^{-1}. \tag{14b}$$

The coefficients a, b and c should be calculated for each model at every frequency channel. We choose these coefficients according to the Kolmogorov - Smirnov criterion, which requires that the cumulative distribution function

$$P(\lambda) = \int_0^\lambda q(\lambda) d\lambda \tag{15}$$

be close to the observed cumulative distribution function. Table 4 gives the "best" values for the coefficients a, b and c for the distribution (14) for the models in eqs. (10), (12) and (13). Having the distribution function of λ, we can predict the duration of strong ground motion which will not be exceeded with any given probability at a site with known properties during an earthquake with

given parameters. For some probability $\bar{P}$, the value of $\lambda_{\bar{P}}$, such that $P(\lambda_{\bar{P}}=\bar{P})$, can be found from eqs. (14)—(15). The duration not to be exceeded with probability $\bar{P}$ is then $dur_{\bar{P}}=dur \cdot \lambda_{\bar{P}}$, where *dur* is the duration of strong motion, predicted by the model we have chosen.

DISCUSSION

The models presented in this paper serve to provide an understanding of the physical mechanism which may be responsible for the prolongation of duration of strong ground motion at sites located on sediments. However, the prolongation mechanism described here (reflection of the surface waves at the boundaries of the valleys back inside the valleys) is only one possible way to interpret these observations.

Consider for example the case shown in figure 4. The earthquake source generates the body (and the surface) seismic waves. Some body waves penetrate deep into the crust and reach the recording station from below. Some body waves are converted into surface waves at the first boundary rock – sediments, at the distance ρ_1' from the source. Together with the surface waves generated in the epicentral region, these waves propagate through the sedimentary valley and reach the boundary at the epicentral distance $\rho_1'+p_1'$, where they partially reflect back into the valley (this surface wave energy is "trapped" in the valley) and partially continue to propagate away from the source in the form of body and surface waves. Similar processes of surface – body wave conversions and reflections from the edges of the valley repeats itself in each sufficiently deep alluvial valley. As a result, a complex picture of overlapping strong motion pulses consisting of body and surface waves is recorded at the station.

When the 3 – dimensional geometry of the region of wave propagation is irregular and so many factors contribute to the formation of the signal at the location of the station, it is difficult to decide how to describe these factors using just a few parameters which can be included into regression analysis. For example, we considered the percentage of epicentral distance covered by rocks on the earth's surface, $\xi=(\rho_1'+\rho_2')/\Delta$, and looked at $\tau_\Delta=(a_4^{(1)}+a_4^{(2)}\xi)\cdot\Delta$ instead of $\tau_\Delta=a_4\cdot\Delta$ in eq. (1) (Novikova and Trifunac, 1993a). It appears that, per each 10 km of epicentral distance at frequencies near 0.3 Hz, duration is prolonged by 2.5 sec if $\xi=0$ (the direct surface straight path from the source to the station does not cross any rocks, and by only 0.8 sec if $\xi=0$ (the epicenter and the station are located in the same rock outcrop). We explained this by stronger dispersion expected along more "alluvial" path than along "rocky" path.

Choosing ξ as one of the parameters describing the geometry of the region where the strong motion is observed is, however, only and approximation. If the deep source and the recording station are separated by several valleys, the main strong motion energy observed at the site could be coming from the direct body waves and from the surface waves generated at the edges of the valley where the station is located. In this case, one can choose to consider the percentage of path covered by alluvium valleys which effectively participate in the carrying surface waves energy to the recording site and exclude the valleys located far from the station. If the source in figure 4 is shifted to a deeper depth, this parameter can be expressed as the ratio ρ_2'/Δ.

Another parameter, probably useful in consideration of shallow sources, is the number of boundaries rock – sediments and sediments – rock crossed by the seismic waves on their way to the

recording station. It may influence not only the duration of strong motion, but also the amplitude of Fourier spectrum observed at the site. Large number of boundaries should weaken the signal. Also, the large number of valleys reduce the amplitudes of strong motion because some energy is "trapped" in these valleys and never comes to the recording station.

The influence of all these and of other parameters on the strong motion characteristics would be interesting to study. However, the possibilities to detect the influence of the associated parameters strongly depend on the available database. If there are not enough cases for each value of a discrete parameter or for each (reasonably small) range of values for a continuous parameter, its influence cannot be detected even if it is significant. To this end, we should consider a parameter, describing the prolongation of duration in alluvial valleys, which is different from those discussed in this paper ("reflection distance" R, depth of sediments h and "reflection angle" φ) and which may be represented by our database (figure 12). This is the distance from the station (located in a valley) to the edge of the valley, where the body waves are likely to generate the surface waves (Vidale and Helmberger, 1988), This parameter, l, could be measured for 226 records from our database (figure 12).

When the limitations of our modeling the prolongation of duration, as it is described in this paper are understood, the results of this work can be used for the prediction of the duration expected during future earthquakes, when the parameters of the shock (M and Δ) and the site (R, φ and h) can be specified. However, we note that our equations (with the coefficients shown in talbes 1—4) can be employed for such prediction in the region where the data, used in the regression analysis, were recorded (Western U. S. , and primarily Southern California). A different geological environment may change the prevailing earthquake mechanism, the distribution of hypocentral depths of the sources, the velocities and the attenuation factors, thus changing values of the regression coefficients.

ACKNOWLEDGEMENTS

This work was supported in part by the California Department of Transportation and the City and County of Los Angeles, through the Southern California Earthquake Center. This support is gratefully acknowledged.

REFERENCES

Hauksson, E. , T. Teng, and T. L. Henyey (1987). Results from a 1500m Deep, Three - Level Downhole Seismometer Array: Site Response, Low Q Values, and f_{max}, *Bull. Seism. Soc. Amer.* , 77, 1883 - 1904.

Lee, V. W. (1991). Correlation of Pseudo Relative Velocity Spectra with Site Intensity, Local Soil Classification and Depth of Sediments, *Int. J. Soil Dyn. Earthquake Eng.* , 10. 141—151.

Lee, V. W., and M. D. Trifunac (1987). Strong Earthquake Ground Motion Data in EQINFOS: Part I, *Dept. of Civil Eng.*, *Report No.* 87 - 01, *Univ. of Southern Calif.*, Los Angeles, California.

Levander, A. R. (1990). Seismic Scattering Near the Earth's Surface, *Pure Appl. Geophys.*, 132, 21 - 47.

Malin, P. E., J. A. Waller, R. D. Bordcherdt, E. Cranswick, E. G. Jensen, and J. Van Schaack (1988). Vertical Seismic Profiling of Oroville Micro Earthquakes: Velocity Spectra and Particle Motion as a Function of Dept., *Bull. Seism. Soc. Amer.*, 78, 401 420.

McCann, M. W., and H. C. Shah (1979). Determining Strong - Motion Duration of Earthquakes, *Bull. Seism. Soc. Amer.*, 69, 1253 - 1265.

Moeen Vaziri, N., and M. D. Trifunac (1988a). Scattering and Diffraction of Plane SH Waves by Two - Dimensional Inhomogeneities: Part I, *Int. J. Soil Dyn. Earthquake Eng.*, 7, 179–188.

Moeen - Vaziri, N., and M. D. Trifunac (1988b). Scattering and Diffraction of Plane P and SV - Waves by Two - Dimensional Inhomogeneities: Part I, *Int. J. Soil Dyn. Earthquake Eng.*, 7, 189–200.

Novikova, E. I., and M. D. Trifunac (1993a). Duration of Strong Ground Motion: Physical Basis and Empirical Equations. *Dept. of Civil Eng.*, *Report No.* 93–02, *Univ. of Southern Calif.*, Los Angeles, California.

Novikova, E. I., and M. D. Trifunac (1993b). Modified Mercalli Intensity Scaling of the Frequency Dependent Duration of Strong Ground Motion. *Soil Dyn. and Earthquake Eng.* (in press).

Novikova, E. I., and M. D. Trifunac (1993c). The Modified Mercalli Intensity and the Geometry of the Sedimentary Basin as Scaling Parameters of the Frequency Dependent Duration of Strong Ground Motion. *Soil Dyn. and Earthquake Eng.* (in press).

Page, R. A., D. M. Boore, W. B. Joyner, and H. W. Coulter (1972). Ground Motion Values for Use in the Seismic Design of the Trans - Alaska Pipeline System, *USGS Circular* 672.

Press, W. H., B. P. Flannery, S. A. Teukolsky, and W. T. Vetterling (1986). Numerical Recipes, Cambridge University Press, U. S, A.

Smith, M. B. (1964) Map Showing Distribution and Configuration of Basement Rocks in *California* (North Half) (South Half), Oil and Gas Investigations, *Map OM* - 215, *Dept. of the Interior United States Geological Survey*, Washington, D. C.

Todorovska, M. I., and V. W. Lee (1990). A Note on Response of Shallow Circular Valleys to Rayleight Waves: Analytical Approach, *Earthquake Eng. and Eng. Vibrations*, 10, 21–34.

Todorovska, M. I., and V. W. Lee (1991a). Surface Motion of Shallow Circular Alluvial Valleys for Incident Plane SH Waves — Analytical Solution, *Int. J. Soil Dyn.*

Earthquake Eng., 10, 192-200.

Todorovska, M. I., and V. W. Lee (1991b). A Note on Scattering of Rayleigh Waves by Shallow Circular Canyons: Analytical Approach, *Bull. Ind. Soc. of Earthquake Technology*, Paper 306, Vol. 28, No. 2, 1-16.

Trifunac, M. D. (1971a). Response Envelope Spectrum and Interpretation of Strong Ground Motion. *Bull. Seism. Soc. Amer.*, 61, 343-356.

Trifunac, M. D. (1971b). Surface Motion of Semi - Cylindrical Alluvial Valley for Incident SH waves, Bull. Seism. Soc. Amer., 61, 1755-1770.

Trifunac, M. D. (1973) A Note on Scattering of Plane SH Waves by Semi - Cylindrical Canyon, Int. J. Earthquake Eng. Strudural Dyn., Vol. 1, 267-281.

Trifunac, M. D. (1989a). Dependence of Fourier Spectrum Amplitudes of Recorded Strong Earthquake Accelerations on Magnitude, Local Soil Conditions and on Depth of Sediments, *Earthquake Eng. Structural Dyn.*, 18, 999-1016.

Trifunac, M. D. (1989b). Empirical Scaling of Fourier Spectrum Amplitudes of Recorded Strong Earthquake Accelerations in Terms of Magnitude and Local Soil and Geologic Conditions, *Earthquake Eng. and Eng. Vibration*, Vol. 9, No. 2, 23-44.

Trifunac, M. D. (1989C). Scaling Strong Motion Fourier Spectra by Modified Mercalli Intensity, Local Soil and Geologic Site Conditions, *Structural Eng./Earthquake Eng., JSCE*, Vol. 6, No. 2, 217-224.

Trifunac, M. D. (1990). How to Model Amplification of Strong Earthquake Motions by Local Soil and Geological Site Conditions, *Earthquake Eng. Structural Dyn.*, 19, 833 846.

Trifunac, M. D. (1991). Empirical Scaling of Fourier Spectrum Amplitudes of Recorded Strong Earthquake Accelerations in Terms of Modified Mercalli Intensity, Local Soil Conditions, and Depth of Sediments, *Soil Dynamics and Earthquake Eng.*, Vol. 10, No. 1, 65-72.

Trifunac, M. D., and A. G. Brady (1975). On the Correlation of Seismic Intensity Scales with the Peaks of Recorded Strong Ground Motion, *Bull. Seism. Soc. Amer.*, 65, 139 162.

Trifunac, M. D., and V. W. Lee (1990). Frequency Dependent Attenuation of Strong Earthquake Ground Motion, *Int. J. Soil Dyn. Earthquake Eng.*, 9, 3-15.

Trifunac, M. D., and B. D. Westermo (1977). A Note on the Correlation of Frequency Dependent Duration of Strong Earthquake Ground Motion with the Modified Mercalli Intensity and the Geological Conditions at the Recording Stations, *Bull. Seism. Soc. Amer.* 67, 917-927.

Trifunac, M. D., and B. D. Westermo (1982). Duration of Strong Earthquake Shaking, *Int J. Soil Dyn. Earthquake Eng.*, 2, 117-121.

Vanmarcke, E. H., and S. P. Lai (1980). Strong - Motion Duration and Rms Amplitude of Earthquake Records, *Bull. Seism. Soc. Amer.*, 70, 1293-1307.

Vidale, J. E., and D. V. Helmberger (1988). Elastic Finite - Difference Modeling of the 1971

San Fernando Earthquake, *Bull. Seism. Soc. Amer.*, 78, 122-141.

Westermo, B. D., and M. D. Trifunac (1978). Correlations of the Frequency Dependent Duration of Strong Earthquake Ground Motion with the Magnitude,. Epicentral Distance, and the Depth of Sediments at the Recording Site, *Dept. of Civil Eng.*, *Report No.* 78-12, *Univ. of Southern Calif.*, Los Angeles, California.

Westermo, B. D., and M. D. Trifunac (1979). Correlations of the Frequency Dependent Duration of Strong Ground Motion with the Modified Mercalli Intensity and the Depth of Sediments at the Reeording Site, *Dept. of Civil Eng.*, *Report No.* 79 01, *Univ. of Southern Calif.*, Los Angeles, California.

Wong, H. L., and M. D. Trifunac (1974a). Scattering of Plane SH Waves by a Semi Elliptical Canyon. *Int. J. Earthquake Eng. Structural Dyn.*, Vol. 3, 157-169.

Wong. H. L,. and M. D. Trifunac (1974b). Surface Motion of Semi - Elliptical Alluvial Valley for Incident Plane SH - Waves, *Bull. Seism. Soc. Amer.*, 64, 1389-1408.

Figure Captions

Figure 1 Number of 3-component records in which at least one channel in at least one component of acceleration, velocity or displacement was accepted (as a noise free)for use in the regression analysis: a) as a function of earthquake magnitude, b) as a function of the epicentral distance.

Figure 2 Distribution of the 3-component records of good quality (at least one component of acceleration, velocity or displacement in at least one channel was adopted for use in the regression analysis) with respect to: a) earthquake magnitude, b) epicentral distance.

Figure 3 The definition of duration illustrated for the east acceleration component of the Morgan Hill earthquake, band - pass filtered by channel #4 filters (central frequency 0.37 Hz):

a) time history f(t) with strong motion intervals (shaded);

b) $\int_0^t f^2(\tau)d\tau$ and its smoothed version;

c) the derivative of the smoothed integral of $f^2(t)$ and its threshold level ρ_μ. The time intervals giving contribution to duration with $\mu=0.9$ are highlighted.

Figure 4 A scheme of wave propagation pattern. The strong motion energy reaches the station in form of the surface waves, some of which are generated at the edge of the valley (at the distance $\rho_1'\rho_1'+\rho_2'$ from the epicenter) and in the form of body waves, coming to the station from below (of course, many other forms of wave propagation are possible). Some of the seismic energy remains "trapped" in the first valley (of the horizontal size ρ_1') and never reaches the recording site located in the second valley. The distances ρ_i' stand for the portion of the epicentral distance covered by rocks ($x=r$) or by sediments ($x=s$).

Figure 5 An idealized representation for the definition of the generalized parameters R and φ. "1" represents the basement rocks, appearing on the earth's surface. "2" shows the angle, subtended at the source by the rocks from which reflection occurs, with the solid lines representing the

direct waves, emitted by the source towards the rocks. "3" gives the symbol for the angle, subtended at the recording station by the surface of the rocks from which reflection occurs, with the dashed lines representing the waves reflected by the rock towards the station. For the i^{th} rock, r_i is the distance from the source to the rock, R_i is the distance from the rock to the station, amd φ_i is the angle, subtended at the station by the rock.

Figure 6 Determination of the parameters for the horizontal reflections (the angle φ, subtended at the recording station by the surface of the rocks from which reflections occur, and the characteristic horizontal distance to these rocks, R) for the Livermore earthquake, of January 26, 1980, recorded in the San Francisco bay area. The distribution and configuration of the basement rocks are taken from the Smith's map (1964). With the superscript corresponding to the station number, $R^{(1)}=20\text{km}$, $R^{(2)}=30\text{km}$, $R^{(3)}=25\text{km}$, $R^{(4)}=45\text{km}$, $R^{(5)}=45\text{km}$, and $\varphi^{(1)}=70°$, $\varphi^{(2)}=40°$, $\varphi^{(3)}=70°$, $\varphi^{(4)}=40°$, $\varphi^{(5)}=30°$.

Figure 7 Reflection of a wave from the boundary of a sedimentary basin. The station is shown by the black triangle, the direction of wave propagation is represented by the arrows. h is the depth of sediments under the station, R is the distance to the reflecting rock as it is seen on the earth's surface, and R_{eff} is the "effective" distance from the station to the region were the reflection actually occurs.

Figure 8 The regression coefficients of eq. (10), plotted versus the central frequency of the channels (solid lines). The coefficients are bounded by their "σ - intervals" (dashed lines) and by their estimated 95% confidence intervals (dotted lines).

Figure 9 Isolines of the additional (relative to the basement rock sites) duration (in seconds) of strong ground motion due to a specific geometry of the sedimentary basin, as estimated from eq. (10). The positive contribution of the terms $\underline{dur}^{(h)}(R,h)$ and $\underline{dur}^{(v)}(R,h)$ defined by eq. (11) only is considered. The observed duration is shown averaged over the various ranges of R and h, specified by the dashed mesh. Longer duration corresponds to a darker shade. The horizontal and the vertical components are shown separately for each channel. The scale of shades, however, is the same for both types of components. For moderate frequencies, longer duration can be seen for intermediate values of R (25÷55 km) and h (2÷5 km).

Figure 10 Additional (relative to basement rock sites) duration (in seconds) due to the specific horizontal characteristic dimension of the sedimentary valley, R as predicted by eq. (12): a) horizontal component, b) vertical component. This "truncated" model preserves the main features of the "complete" model (eq. (10)) regarding the behavior of the terms which describe the prolongation of the duration due to the specific geometry of the sedimentary basin.

Figure 11 Additional (relative to basement rock sites) duration (in seconds) due to the depth of sediments under the recording site, h, as predicted by eq. (13): a) horizontal component; b) vertical component. This "truncated" model preserves the main features of the complete model (eq. (10)). regarding the behavior of the terms which describe the prolongation of the duration due to the specific geometry of the sedimentary basin.

Figure 12 Distribution of records in our database with respect to the mutual location of the earthquake source, recording station and the sedimentary valleys in the area of strong ground

shaking. R is the "reflection distance"defined in figures 5 and 7, l is the distance from the station to the edge of the valley where the surface waves are likely to be generated from the body waves when the latter enter the sedimentary basin.

Table Captions

Table 1 Results of the regression analysis of eq. (10).

Table 2 Results of the regression analysis of eq. (12).

Table 3 Results of the regression analysis of eq. (13).

Table 4 Coefficients of the distribution function $q(\lambda)$ (see eq. (14)) for the models (10), (12) and (13).

Table 1

Channel number	f_0 (Hz)	# of data points N(f)	Coefficients a_i and their accuracy ("σ-interval")																M_{min}	σ_{dur} (sec)	dur_{av} (sec)
			$a_1^{(h)}$ $\pm\sigma_1^{(h)}$	$a_1^{(v)}$ $\pm\sigma_1^{(v)}$	a_2 $\pm\sigma_2$	a_3 $\pm\sigma_3$	a_4 $\pm\sigma_4$	$a_5^{(h)}$ $\pm\sigma_5^{(h)}$	$a_6^{(h)}$ $\pm\sigma_6^{(h)}$	$a_7^{(h)}$ $\pm\sigma_7^{(h)}$	$a_8^{(h)}$ $\pm\sigma_8^{(h)}$	$a_9^{(h)}$ $\pm\sigma_9^{(h)}$	$a_{10}^{(h)}$ $\pm\sigma_{10}^{(h)}$	$a_5^{(v)}$ $\pm\sigma_5^{(v)}$	$a_6^{(v)}$ $\pm\sigma_6^{(v)}$	$a_7^{(v)}$ $\pm\sigma_7^{(v)}$	$a_8^{(v)}$ $\pm\sigma_8^{(v)}$	$a_9^{(v)}$ $\pm\sigma_9^{(v)}$	$a_{10}^{(v)}$ $\pm\sigma_{10}^{(v)}$			
1	0.075	37	40.8 ±2.0	32.5 ±3.1	0	0	0	0	0	0	0	0	0	0	0	0	0	0		10.2	38.3
2	0.12	311	19.1 ±1.1	19.4 ±1.6	0	0	.191 ±.019	0	0	0	0	0	0	0	0	0	0	0		10.2	28.3
3	0.21	962	11.9 ±0.6	13.6 ±0.7	.0	.0	.215 ±.012	.0	.0	.0	.0	.0	.0	.0	.0	.0	.0	.0		8.0	21.4
4	0.37	1381	5.8 ±3.4	6.8 ±3.5	.84 ±.54	.0	.196 ±.009	.0	.0	.0	.0	.0	.0205 ±.0045	.0	.0	.0	.0	.0	.0169 ±.0075		7.3	20.9
5	0.63	1219	-5.8 ±2.8	-2.4 ±3.1	2.04 ±.46	.0	.200 ±.009	0	.458 ±.057	.0389 ±.0111	-.0075 ±.0008	-.42 ±.08	.0174 ±.0061	59 ±1.15	245 ±.109	.0638 ±.0192	-.0054 ±.0016	-.65 ±.17	.0224 ±.0107		7.9	19.7
6	1.1	1550	-7.2 ±1.7	-4.2 ±1.9	2.01 ±.32	.0	.166 ±.006	.56 ±.54	.382 ±.051	.0348 ±.0089	-.0070 ±.0007	-.41 ±.09	.0224 ±.0044	.95 ±.78	.142 ±.075	.0607 ±.0143	-.0039 ±.0011	-.59 ±.13	.0209 ±.0073		6.7	16.3
7	1.7	1865	-4.3 ±1.0	-1.9 ±1.2	1.63 ±.21	.0	.134 ±.005	.89 ±.41	.201 ±.038	.0232 ±.0068	-.0040 ±.0006	-.34 ±.07	.0082 ±.0032	1.52 ±.60	.105 ±.055	.0267 ±.0106	-.0024 ±.0008	-.44 ±.10	.0		5.4	13.3
8	2.5	2005	6.3 ±1.7	7.4 ±1.8	-2.51 ±.66	.36 ±.06	.095 ±.003	0	.142 ±.019	.0142 ±.0041	-.0025 ±.0003	-.11 ±.03	.0053 ±.0020	1.42 ±.37	.089 ±.034	.0083 ±.0063	-.0016 ±.0005	-.28 ±.06	.0	3.49	3.5	9.6
9	4.2	2283	8.4 ±1.5	9.9 ±1.5	-3.74 ±.56	.52 ±.05	.076 ±.003	.0	.059 ±.012	.0	-.0006 ±.0002	.0	.0027 ±.0014	.96 ±.26	.0	.0	.0	-.12 ±.05	.0	3.60	3.1	7.6
10	7.2	2244	9.2 ±1.1	9.6 ±1.2	-4.52 ±.44	.65 ±.04	.062 ±.003	.0	.0	.0	.0	.0	.0	.32 ±.22	.0	.0	.0	-.04 ±.04	.0	3.48	2.6	6.5
11	13	1572	6.2 ±1.1	6.3 ±1.1	-3.33 ±.42	.52 ±.04	.055 ±.003	.0	.0	.0	.0	.0	.0	.0	.0	.0	.0	.0	.0	3.20	2.0	5.1
12	21	724	10.1 ±2.1	10.1 ±2.1	-4.68 ±.84	.62 ±.08	.056 ±.007	.0	.0	.0	.0	.0	.0	.0	.0	.0	.0	.0	.0	3.77	1.8	4.2
			I horiz	I vert	M	M^2	Δ	h	R	hR	R^2	h^2	φ	h	R	hR	R^2	h^2	φ			
								horizontal component						vertical component								
			Corresponding parameters																			

Table 2

Channel number	f_0 (Hz)	# of data points N(f)	Coefficients a_i and their accuracy ("σ-interval")											M_{min}	σ_{dur} (sec)	dur_{av} (sec)
			$a_1^{(h)}$ $\pm\sigma_1^{(h)}$	$a_1^{(v)}$ $\pm\sigma_1^{(v)}$	a_2 $\pm\sigma_2$	a_3 $\pm\sigma_3$	a_4 $\pm\sigma_4$	$a_6^{(h)}$ $\pm\sigma_6^{(h)}$	$a_8^{(h)}$ $\pm\sigma_8^{(h)}$	$a_{10}^{(h)}$ $\pm\sigma_{10}^{(h)}$	$a_6^{(v)}$ $\pm\sigma_6^{(v)}$	$a_8^{(v)}$ $\pm\sigma_8^{(v)}$	$a_{10}^{(v)}$ $\pm\sigma_{10}^{(v)}$			
1	0.075	37	40.8 ±2.0	32.5 ±3.1	.0	.0	.0	.0	.0	.0	.0	.0	.0		10.2	38.3
2	0.12	311	19.1 ±1.1	19.4 ±1.6	.0	.0	.191 ±.018	.0	.0	.0	.0	.0	.0		10.2	28.3
3	0.21	962	11.9 ±0.6	13.6 ±0.7	.0	.0	.215 ±.012	.0	.0	.0	.0	.0	.0		8.1	21.4
4	0.37	1381	5.2 ±3.4	5.8 ±3.6	.94 ±.54	.0	.195 ±.009	.0	.0	.0206 ±.0045	.093 ±.066	-.0013 ±.0018	.0144 ±.0079		7.3	20.9
5	0.63	1891	-6.2 ±2.2	-4.8 ±2.3	2.01 ±.36	.0	.198 ±.007	.313 ±.033	-.0045 ±.0005	.0201 ±.0039	.285 ±.056	-.0037 ±.0008	.0254 ±.0065		7.3	18.4
6	1.1	2431	-5.2 ±1.3	-2.8 ±1.4	1.61 ±.23	.0	.169 ±.005	.322 ±.024	-.0050 ±.0004	.0216 ±.0029	.204 ±.040	-.0027 ±.0006	.0271 ±.0047		6.2	15.3
7	1.7	2892	-3.0 ±0.8	-0.9 ±0.9	1.27 ±.15	.0	.137 ±.004	.189 ±.018	-.0028 ±.0003	.0095 ±.0021	.165 ±.027	-.0019 ±.0004	.0084 ±.0031		5.0	12.2
8	2.5	3132	6.4 ±1.6	7.8 ±1.6	-2.44 ±.60	.35 ±.06	.094 ±.003	.106 ±.012	-.0015 ±.0002	.0047 ±.0014	.122 ±.018	-.0015 ±.0003	.0020 ±.0021	3.49	3.4	9.0
9	4.2	2608	8.5 ±1.4	10.5 ±1.5	-3.88 ±.55	.54 ±.05	.076 ±.003	.060 ±.012	-.0007 ±.0002	.0022 ±.0014	.0	0	.0	3.59	3.1	7.6
10	7.2	2553	9.6 ±1.1	10.1 ±1.1	-4.68 ±.42	.66 ±.04	.064 ±.003	.0	.0	.0	.0	.0	.0	3.55	2.6	6.4
11	13	1572	6.2 ±1.1	6.3 ±1.1	-3.33 ±.42	.52 ±.04	.055 ±.003	.0	.0	.0	.0	.0	.0	3.20	2.0	5.1
12	21	724	10.1 ±2.1	10.1 ±2.1	-4.68 ±.84	.62 ±.08	.056 ±.007	.0	.0	.0	.0	.0	.0	3.77	1.8	4.2
			I horiz	I vert	M	M^2	Δ	R	R^2	φ	R	R^2	φ			
								horizontal			vertical					
			Corresponding parameters													

Table 3

Channel number	f_0 (Hz)	# of data points N(f)	Coefficients a_i and their accuracy ("σ-interval")								M_{min}	σ_{dur} (sec)	dur_{av} (sec)
			$a_1^{(h)}$ $\pm\sigma_1^{(h)}$	$a_1^{(h)}$ $\pm\sigma_1^{(h)}$	a_2 $\pm\sigma_2$	a_3 $\pm\sigma_3$	a_4 $\pm\sigma_4$	$a_5^{(h)}$ $\pm\sigma_5^{(h)}$	$a_9^{(h)}$ $\pm\sigma_9^{(h)}$	$a_5^{(v)}$ $\pm\sigma_5^{(v)}$	$a_9^{(v)}$ $\pm\sigma_9^{(v)}$			
1	0.075	37	40.8 ±2.0	32.5 ±3.1	.0	.0	.0	.0	.0	.0	.0		10.2	38.3
2	0.12	311	19.1 ±1.1	19.4 ±1.6	.0	.0	.191 ±.018	.0	.0	.0	.0		10.2	28.3
3	0.21	962	11.9 ±0.6	13.6 ±0.7	.0	.0	.215 ±.012	.0	.0	.0	.0		8.1	21.4
4	0.37	1499	7.8 ±3.2	8.2 ±3.2	.84 ±.52	.0	.191 ±.008	.0	.0	.0	.0		7.4	21.0
5	0.63	1796	1.3 ±2.1	3.3 ±2.4	1.60 ±.37	.0	.182 ±.008	.0	.0	1.43 ±.84	-.29 ±.14		7.9	18.8
6	1.1	1600	-1.3 ±1.8	0.9 ±1.9	1.63 ±.32	.0	.154 ±.007	1.09 ±.45	-.20 ±.08	1.40 ±.66	-.24 ±.12		7.5	16.6
7	1.7	1916	-3.0 ±1.0	-1.1 ±1.1	1.63 ±.20	.0	.126 ±.005	1.12 ±.33	-.18 ±.06	1.68 ±.47	-.26 ±.09		5.8	13.5
8	2.5	2059	6.0 ±1.8	6.6 ±1.9	-2.23 ±.68	.36 ±.06	.089 ±.003	.22 ±.21	-.02 ±.04	1.21 ±.30	-.18 ±.05	3.10	3.9	9.8
9	4.2	2389	8.5 ±1.4	9.1 ±1.5	-3.73 ±.55	.55 ±.05	.070 ±.003	.0	.0	.95 ±.28	-.12 ±.05	3.39	3.2	7.6
10	7.2	2244	9.2 ±1.1	9.6 ±1.2	-4.52 ±.44	.65 ±.04	.062 ±.003	.0	.0	.32 ±.22	-.04 ±.04	3.48	2.6	6.5
11	13	1572	6.2 ±1.1	6.3 ±1.1	-3.33 ±.42	.52 ±.04	.055 ±.003	.0	.0	.0	.0	3.20	2.0	5.1
12	21	724	10.1 ±2.1	10.1 ±2.1	-4.68 ±.84	.62 ±.08	.056 ±.007	.0	.0	.0	.0	3.77	1.8	4.2
			1 horiz	1 vert	M	M^2	Δ	h	h^2	h	h^2			
								horizontal		vertical				
			Corresponding parameters											

Table 4

Ch. number	f_0 (Hz)	For eq.(10)			For eq.(12)			For eq.(13)		
		a	b	c	a	b	c	a	b	c
1	0.075	2.3	3.5	12.0	2.3	3.5	12.0	2.3	3.5	12.0
2	0.12	0.7	2.6	7.6	0.7	2.6	7.6	0.7	2.6	7.6
3	0.21	0.4	2.9	7.1	0.4	2.9	7.1	0.4	2.9	7.1
4	0.37	1.3	2.3	8.6	1.3	2.6	8.7	1.5	2.4	8.6
5	0.63	1.1	1.9	6.9	2.0	1.6	7.3	2.0	1.5	7.0
6	1.1	1.2	1.8	6.9	2.2	1.6	7.4	1.0	1.5	6.0
7	1.7	1.7	1.9	7.8	1.9	1.9	7.7	1.5	1.7	7.1
8	2.5	2.1	1.9	7.5	2.3	1.8	7.6	1.8	1.8	7.3
9	4.2	2.4	1.7	7.3	2.7	1.5	7.2	2.8	1.5	7.3
10	7.2	2.7	1.5	7.1	2.8	1.5	7.2	2.7	1.5	7.1
11	13	3.0	1.5	7.3	3.0	1.5	7.3	3.0	1.5	7.3
12	21	6.6	1.2	7.9	6.6	1.2	7.9	6.6	1.2	7.9

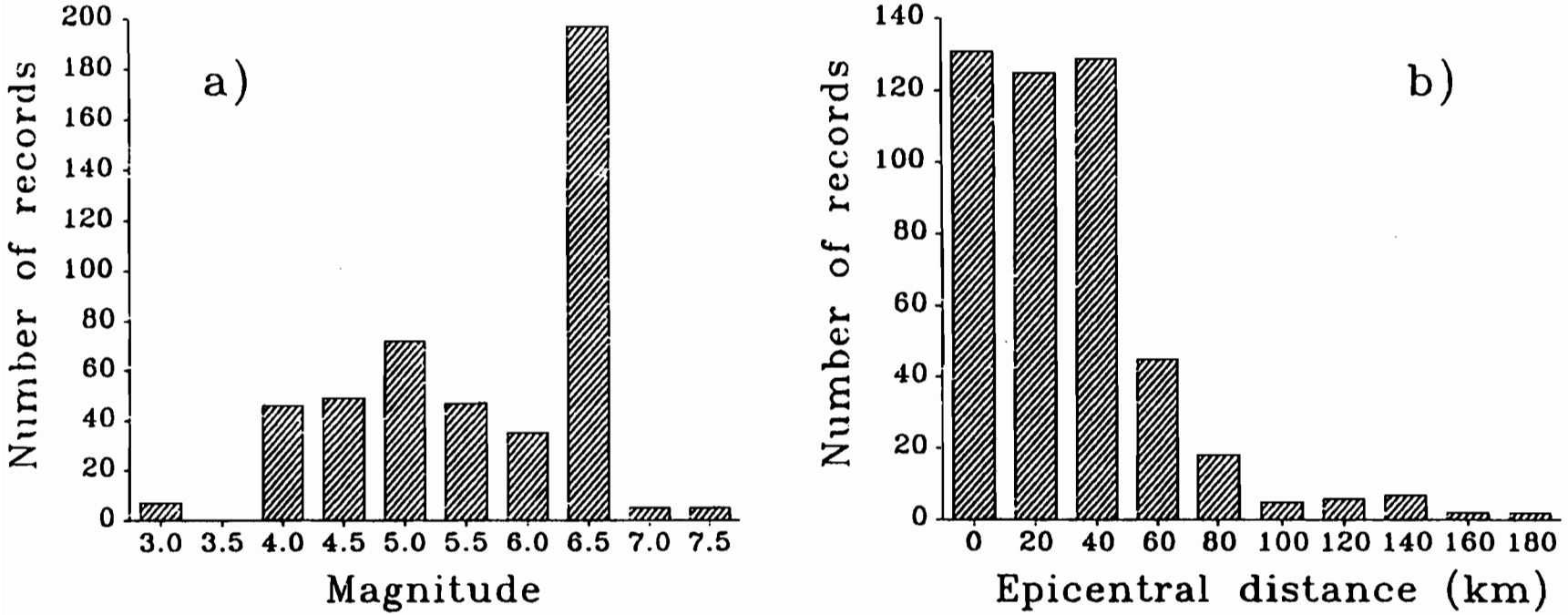
a)
Number of records
200
180
160
140
120
100
80
60
40
20
0
3.0 3.5 4.0 4.5 5.0 5.5 6.0 6.5 7.0 7.5
Magnitude
b)
Number of records
140
120
100
80
60
40
20
0
0 20 40 60 80 100 120 140 160 180
Epicentral distance (km)

Fig. 1

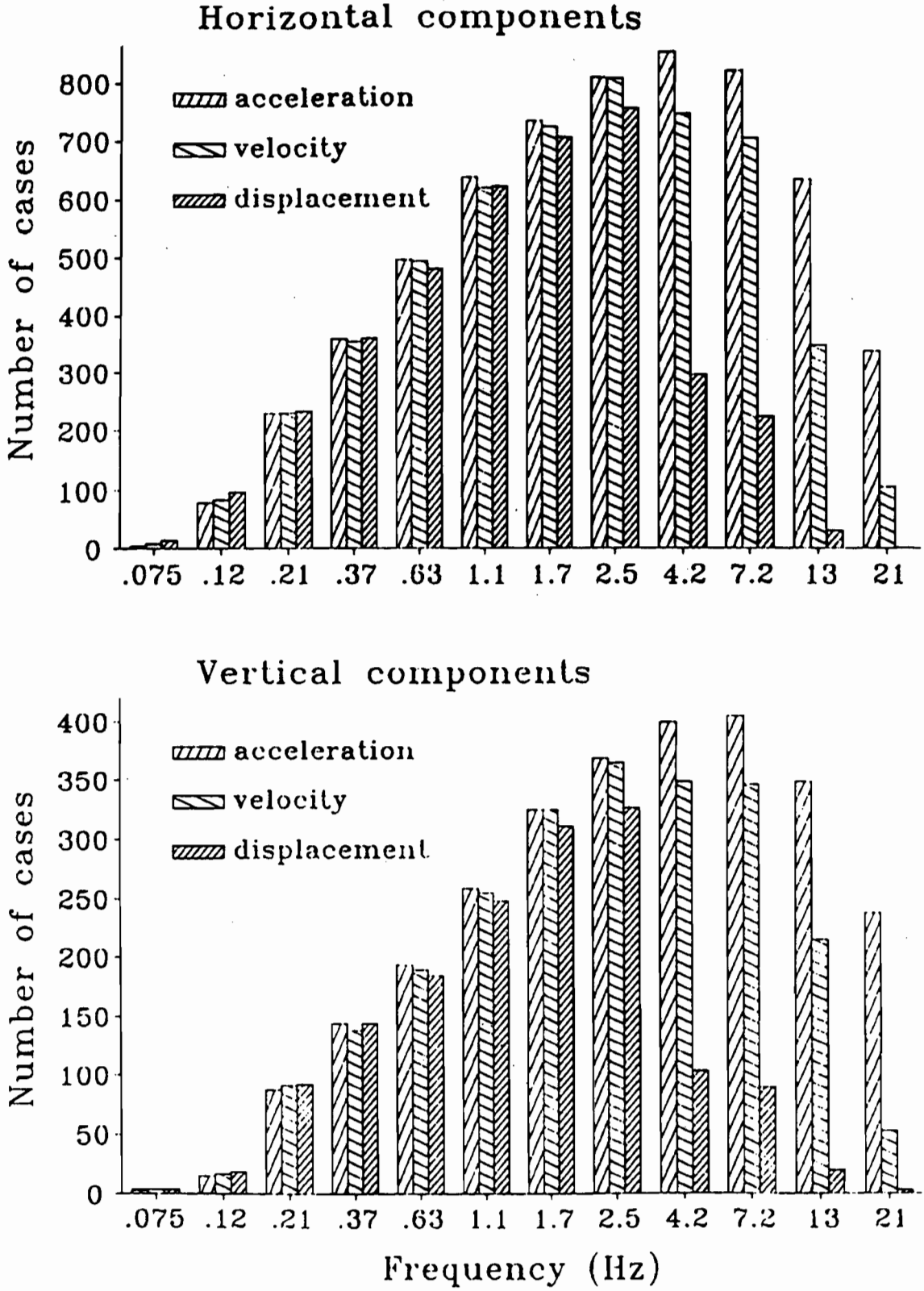
Horizontal components
acceleration
velocity
displacement
Number of cases
0
100
200
300
400
500
600
700
800
.075 .12 .21 .37 .63 1.1 1.7 2.5 4.2 7.2 13 21
Vertical components
acceleration
velocity
displacement
Number of cases
0
50
100
150
200
250
300
350
400
.075 .12 .21 .37 .63 1.1 1.7 2.5 4.2 7.2 13 21
Frequency (Hz)

Fig. 2

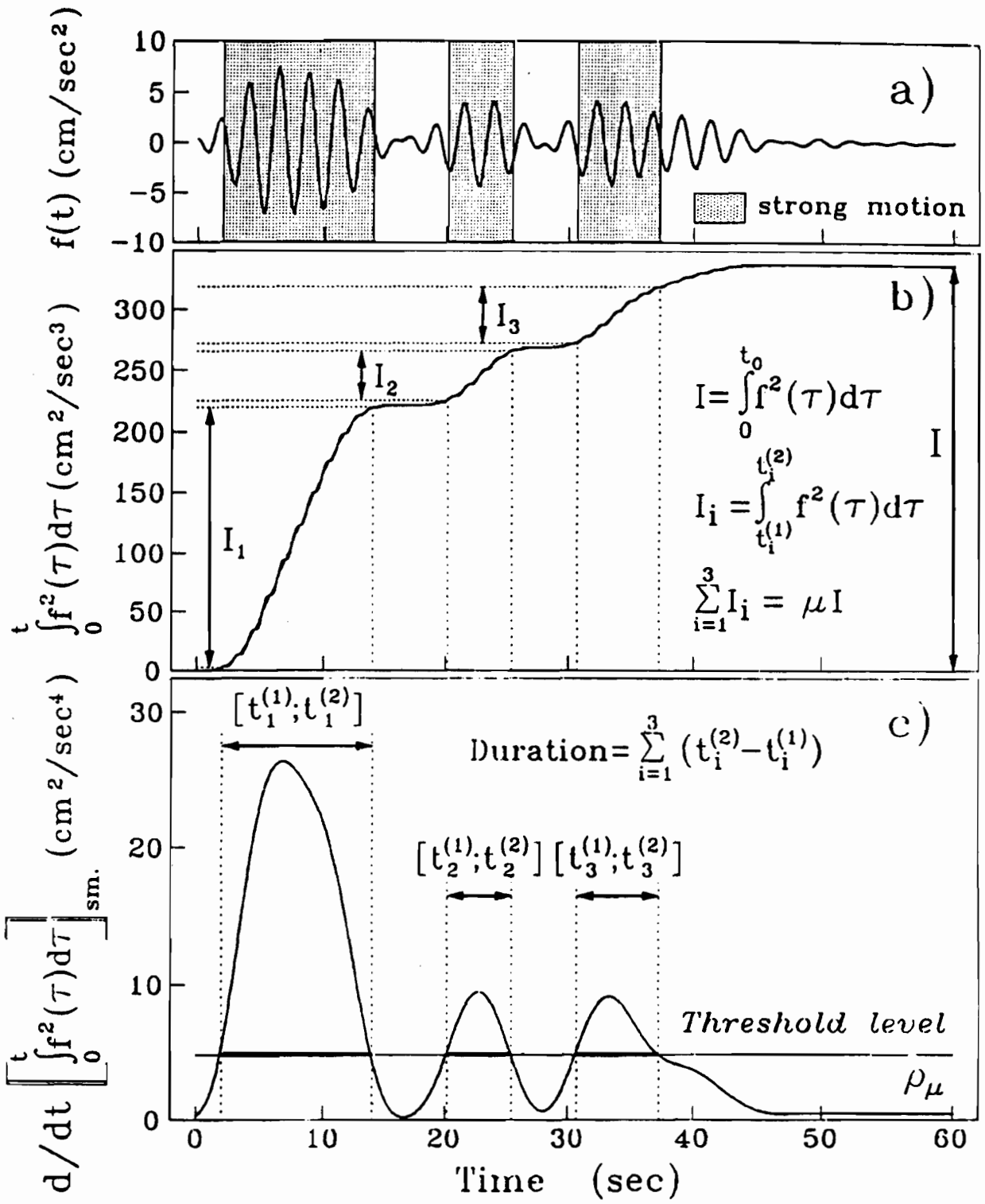
f(t) (cm/sec²)
a)
strong motion
b)
$\int_0^t f^2(\tau)d\tau$ (cm²/sec³)
I_1
I_2
I_3
$I = \int_0^{t_0} f^2(\tau)d\tau$
I
$I_i = \int_{t_i^{(1)}}^{t_i^{(2)}} f^2(\tau)d\tau$
$\sum_{i=1}^{3} I_i = \mu I$
c)
d/dt $\left[\int_0^t f^2(\tau)d\tau\right]_{sm.}$ (cm²/sec⁴)
$[t_1^{(1)}; t_1^{(2)}]$
Duration $= \sum_{i=1}^{3} (t_i^{(2)} - t_i^{(1)})$
$[t_2^{(1)}; t_2^{(2)}]$ $[t_3^{(1)}; t_3^{(2)}]$
Threshold level
ρ_μ
Time (sec)

Fig. 3

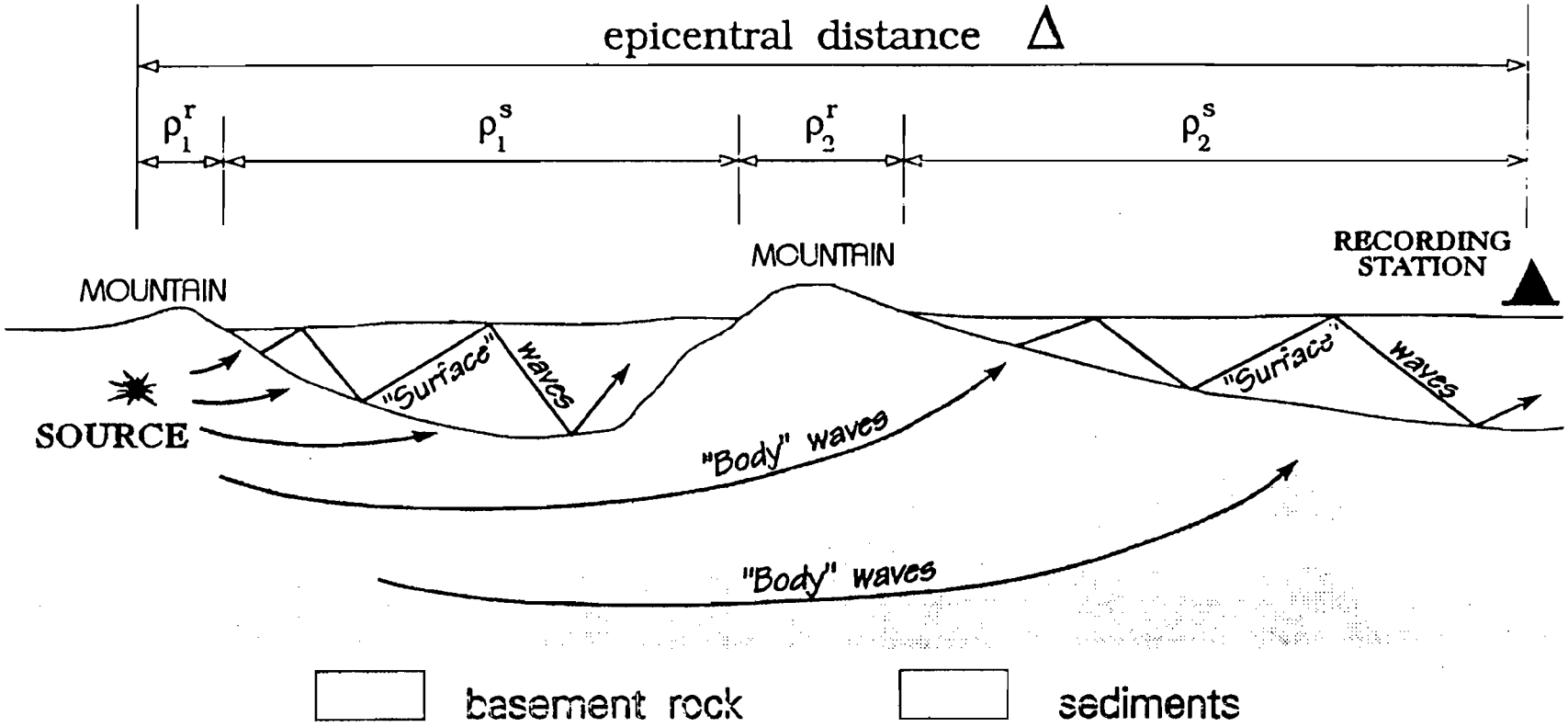
epicentral distance Δ
ρ_1^r
ρ_1^s
ρ_2^r
ρ_2^s
MOUNTAIN
MOUNTAIN
RECORDING STATION
"Surface" waves
"Surface" waves
SOURCE
"Body" waves
"Body" waves
basement rock
sediments

Fig. 4

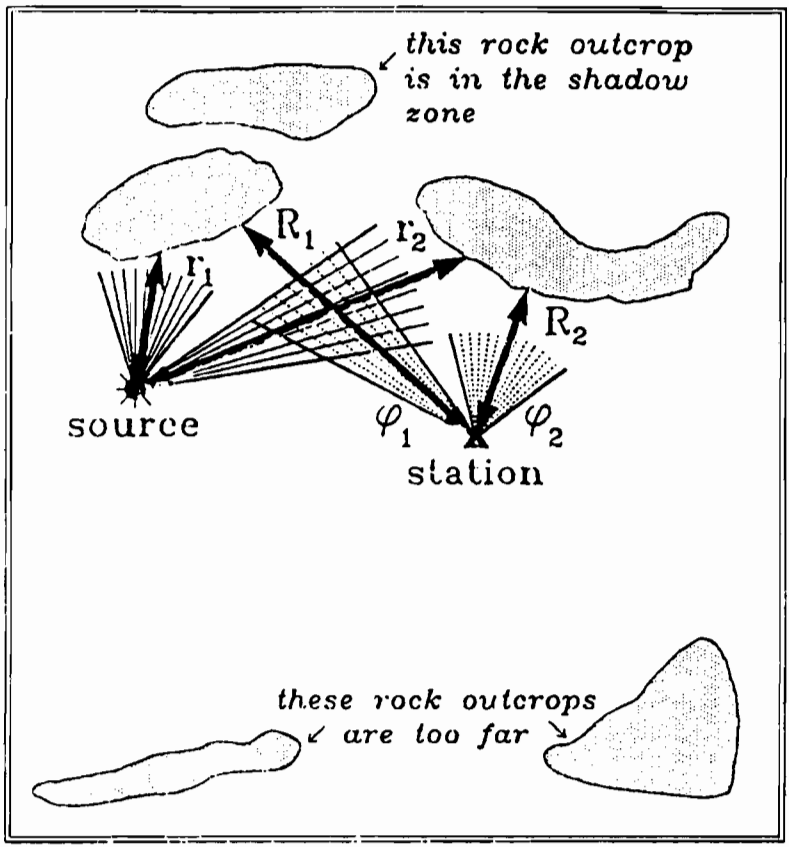
this rock outcrop
is in the shadow
zone
R1
r2
r1
R2
source
φ1
φ2
station
these rock outcrops
are too far
– 1
– 2
– 3

Fig. 5

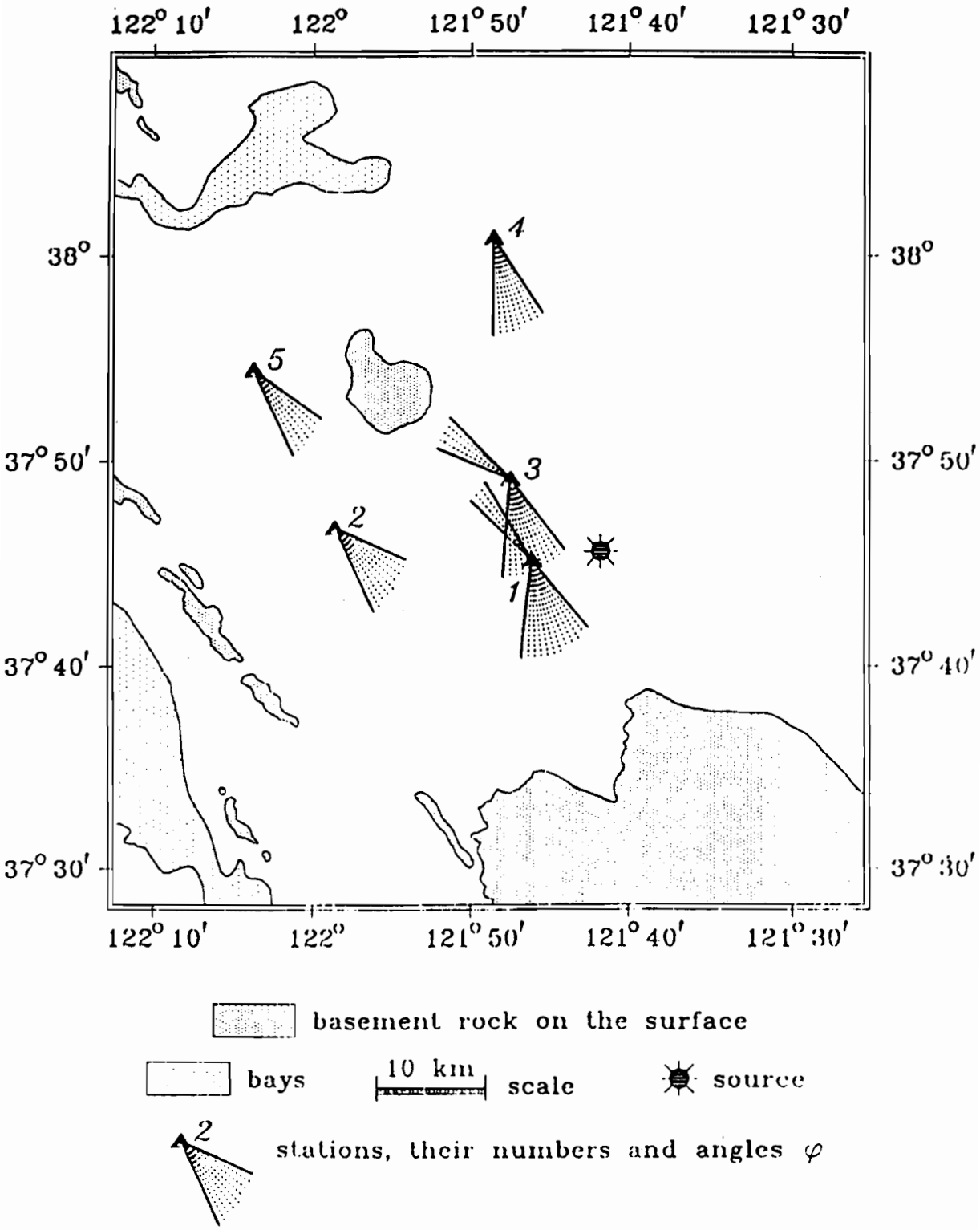
122° 10′
122°
121° 50′
121° 40′
121° 30′
38°
37° 50′
37° 40′
37° 30′
1
2
3
4
5
basement rock on the surface
bays
10 km
scale
source
stations, their numbers and angles φ

Fig. 6

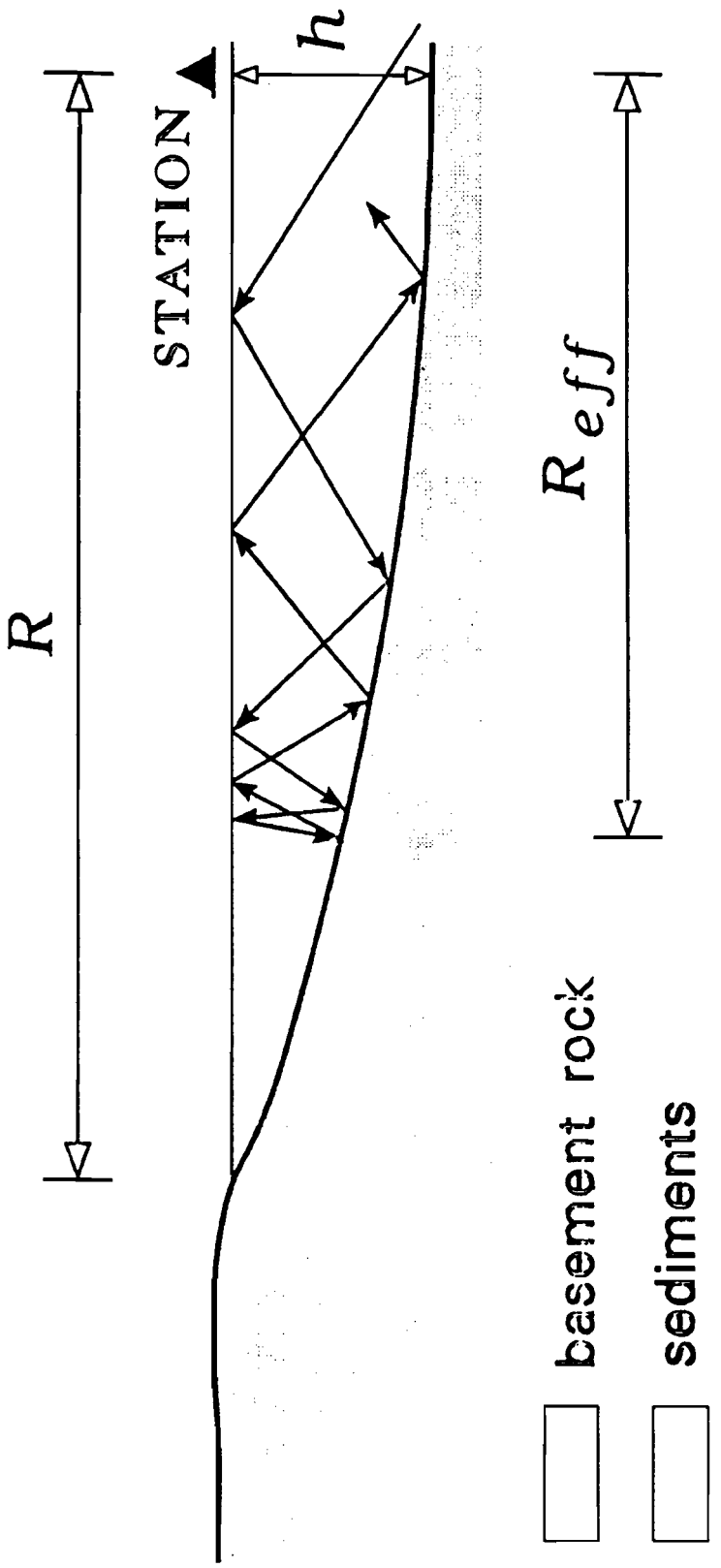

Fig. 7

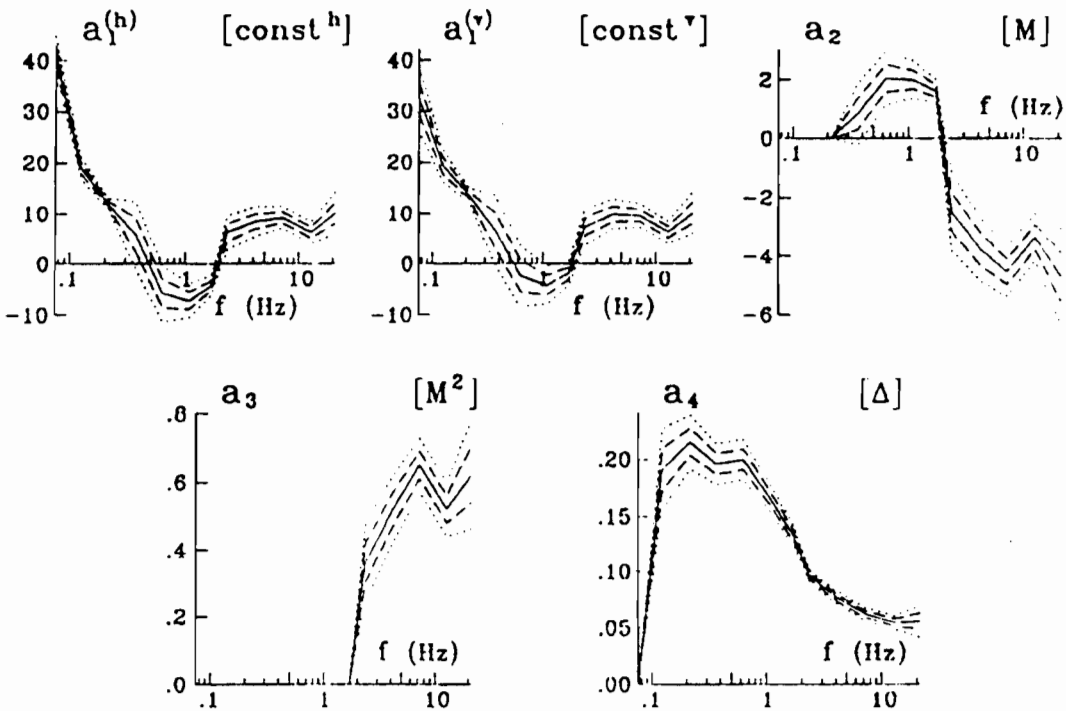
a1(h) [const h]
40
30
20
10
0
-10
.1
1
10
f (Hz)
a1(v) [const v]
40
30
20
10
0
-10
.1
1
10
f (Hz)
a2 [M]
2
0
-2
-4
-6
.1
1
10
f (Hz)
a3 [M2]
.6
.6
.4
.2
.0
.1
1
10
f (Hz)
a4 [Δ]
.20
.15
.10
.05
.00
.1
1
10
f (Hz)

Fig. 8a

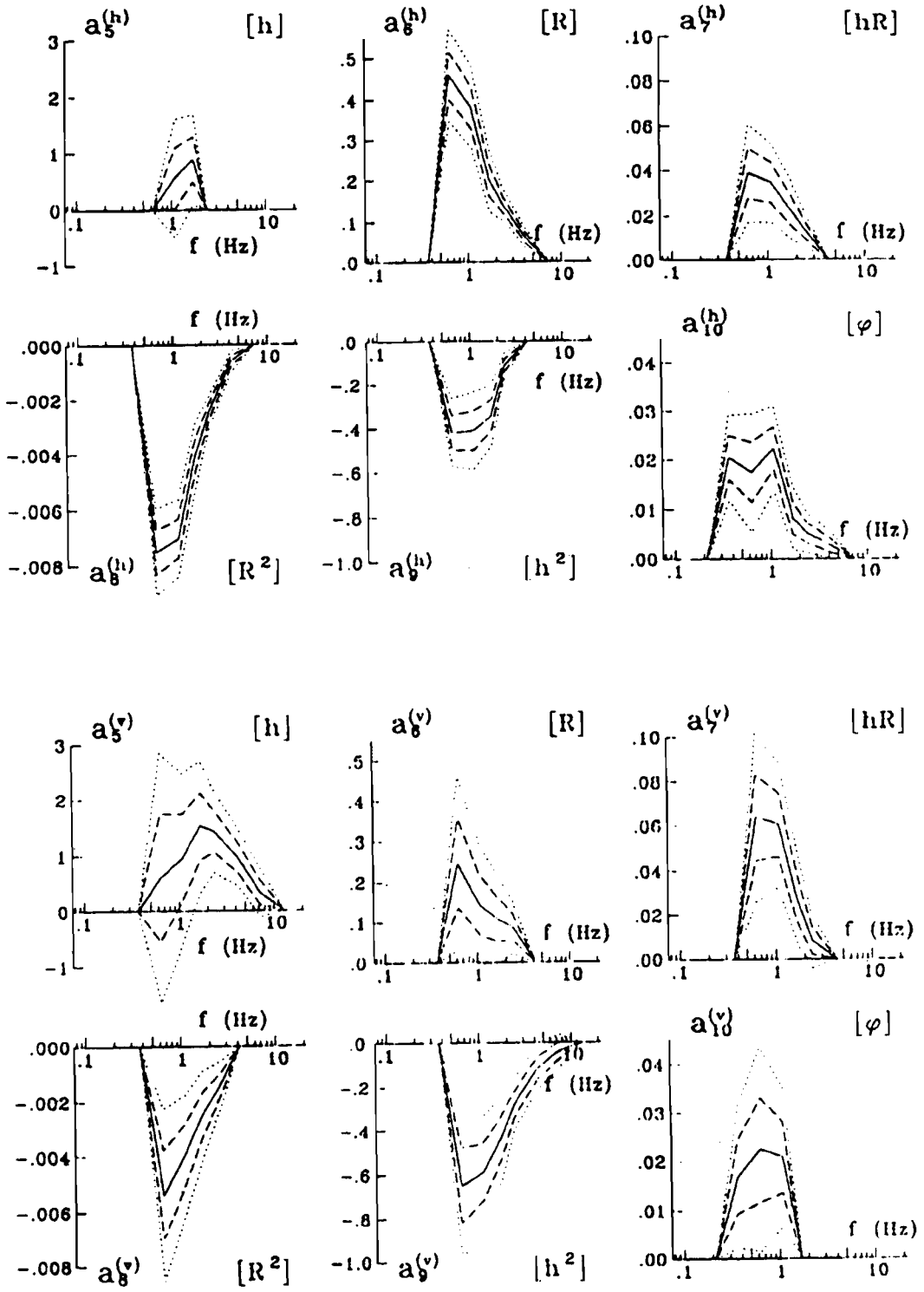
$a_5^{(h)}$ [h]
$a_8^{(h)}$ [R]
$a_7^{(h)}$ [hR]
f (Hz)
$a_8^{(h)}$ [R^2]
$a_9^{(h)}$ [h^2]
$a_{10}^{(h)}$ [φ]
$a_5^{(v)}$ [h]
$a_8^{(v)}$ [R]
$a_7^{(v)}$ [hR]
$a_8^{(v)}$ [R^2]
$a_9^{(v)}$ [h^2]
$a_{10}^{(v)}$ [φ]

Fig. 8b

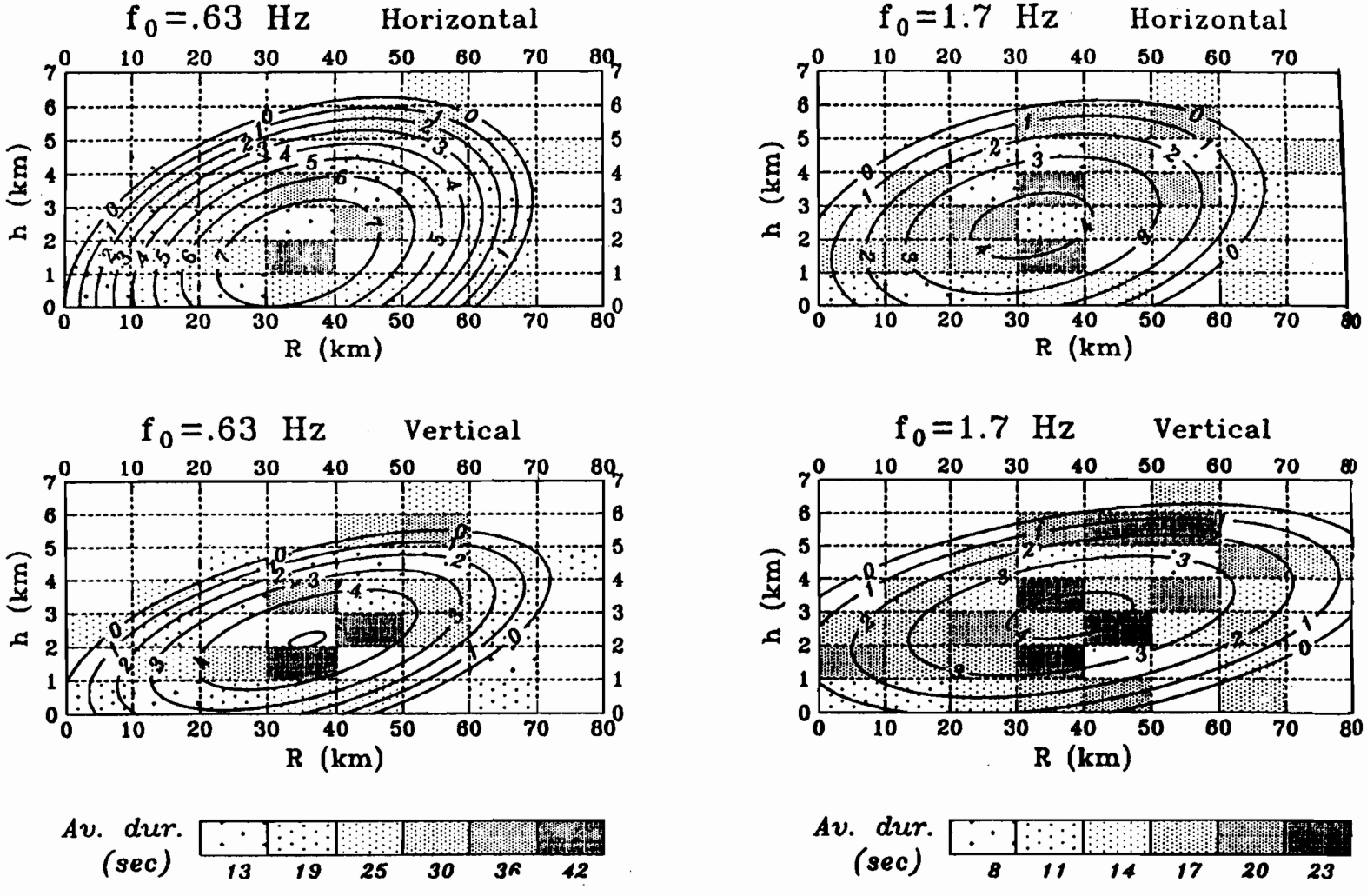
f0=.63 Hz Horizontal
f0=1.7 Hz Horizontal
f0=.63 Hz Vertical
f0=1.7 Hz Vertical
h (km)
R (km)
Av. dur. (sec)
13 19 25 30 36 42
8 11 14 17 20 23

Fig. 9a

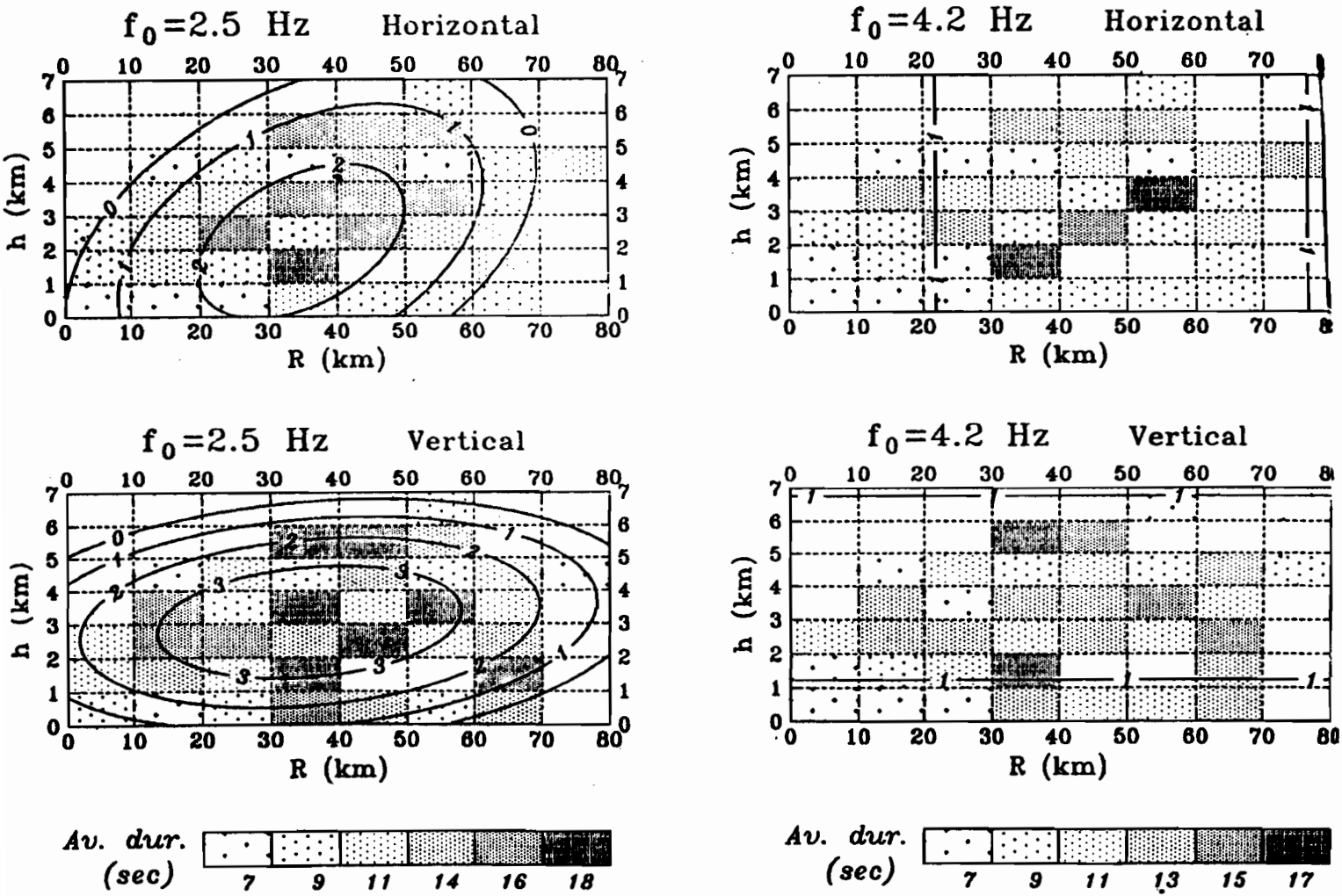
f_0=2.5 Hz Horizontal
f_0=4.2 Hz Horizontal
f_0=2.5 Hz Vertical
f_0=4.2 Hz Vertical
h (km)
R (km)
Av. dur. (sec)
7 9 11 14 16 18
7 9 11 13 15 17

Fig. 9b

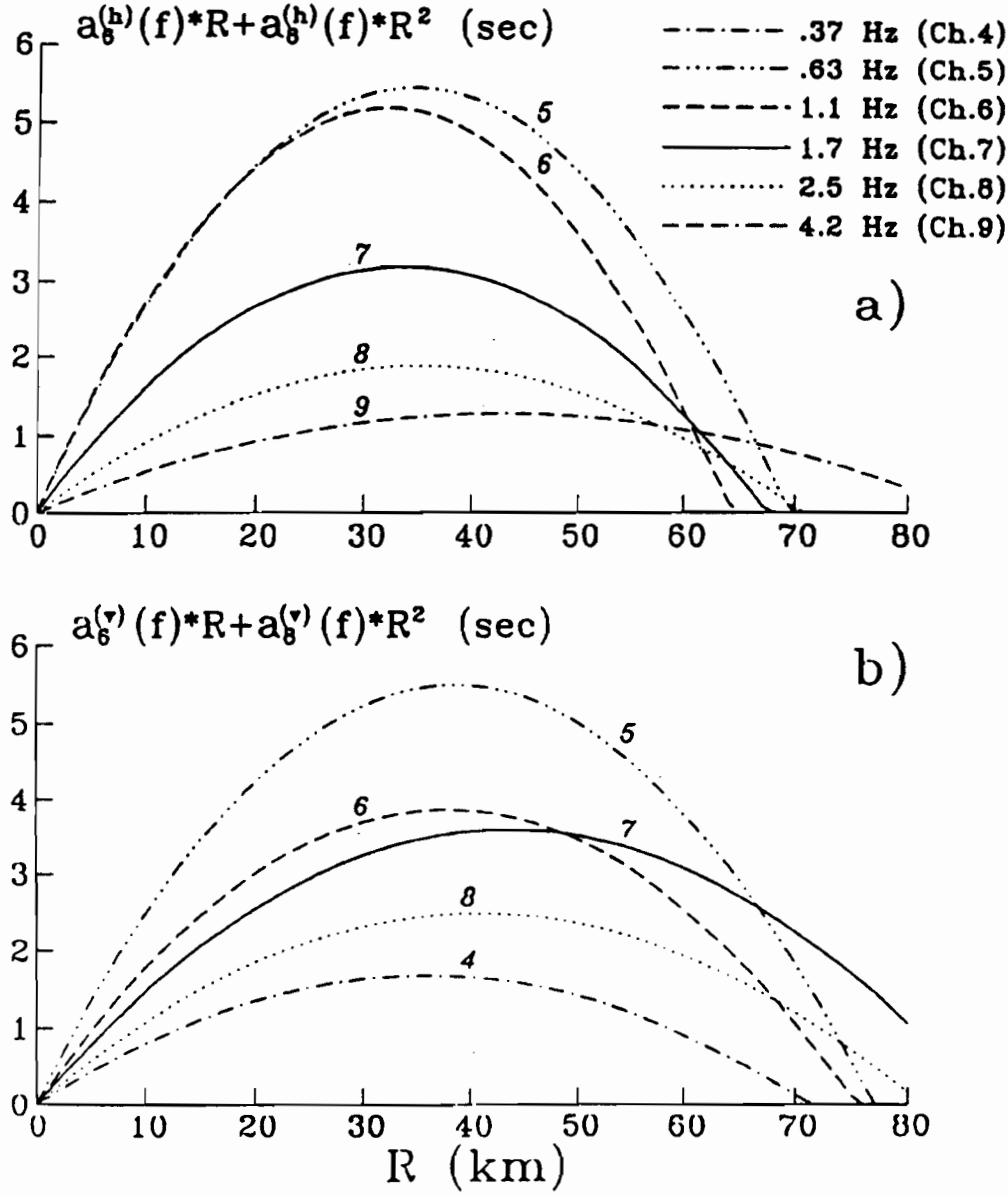
$a_6^{(h)}(f)*R+a_8^{(h)}(f)*R^2$ (sec)
.37 Hz (Ch.4)
.63 Hz (Ch.5)
1.1 Hz (Ch.6)
1.7 Hz (Ch.7)
2.5 Hz (Ch.8)
4.2 Hz (Ch.9)
a)
5
6
7
8
9
$a_6^{(v)}(f)*R+a_8^{(v)}(f)*R^2$ (sec)
b)
5
6
7
8
4
0 10 20 30 40 50 60 70 80
R (km)

Fig. 10

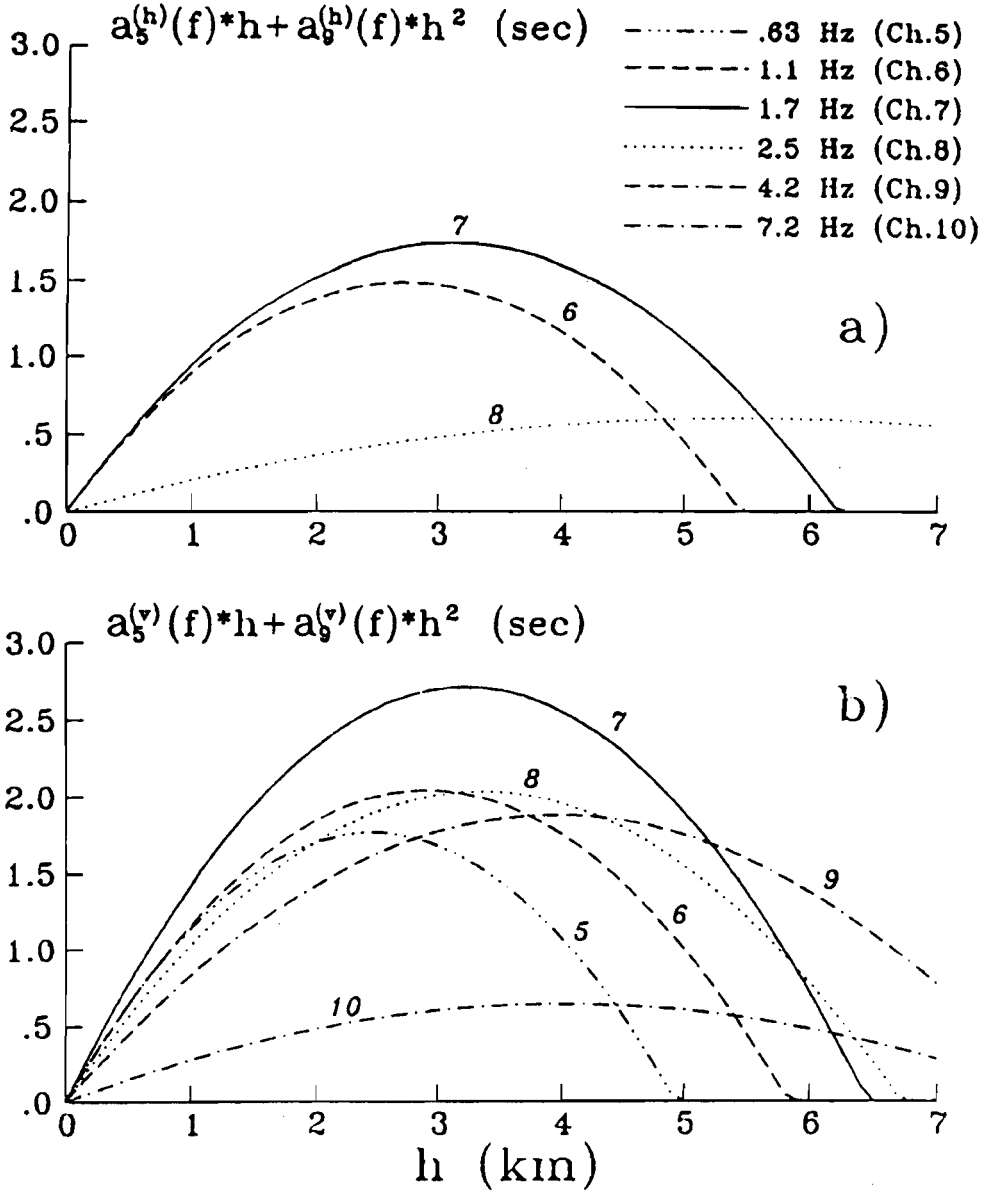
$a_5^{(h)}(f)*h+a_9^{(h)}(f)*h^2$ (sec)
.63 Hz (Ch.5)
1.1 Hz (Ch.6)
1.7 Hz (Ch.7)
2.5 Hz (Ch.8)
4.2 Hz (Ch.9)
7.2 Hz (Ch.10)
a)
$a_5^{(v)}(f)*h+a_9^{(v)}(f)*h^2$ (sec)
b)
h (km)

Fig. 11

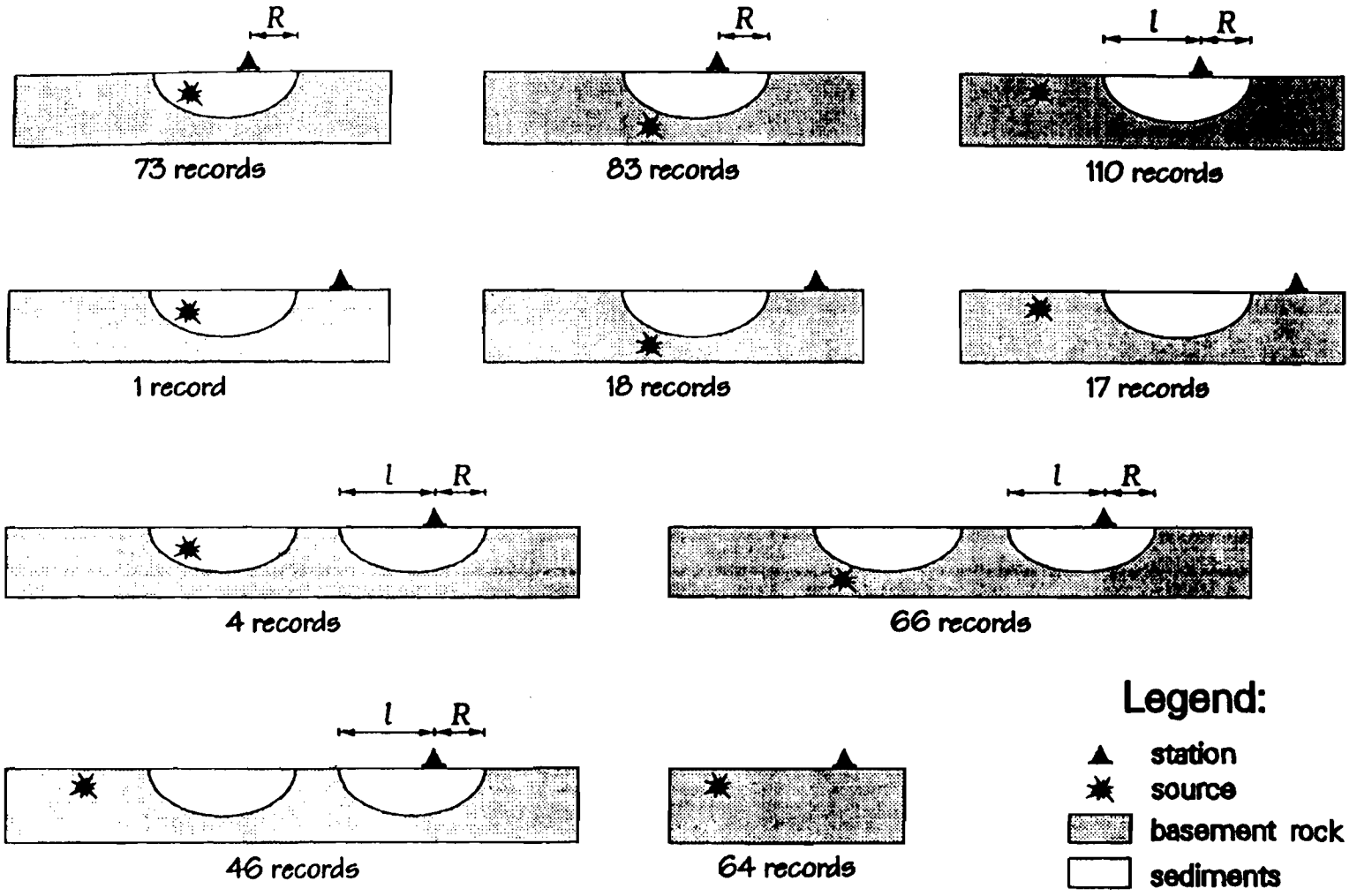
R
73 records
R
83 records
l R
110 records
1 record
18 records
17 records
l R
4 records
l R
66 records
l R
46 records
64 records
Legend:
station
source
basement rock
sediments

Fig. 12